晩期型恒星とその活動
~晩期型恒星の彩層・コロナ~

国 立 天 文 台

渡 邊 鉄 哉

恒星と活動～彩層･コロナ～

- 恒星の磁気活動
- 彩層:水素の電離と熱的分化
  - K(CaII)線（non-LTE line formation）
  - ウィルソン･バップ効果と彩層の尺度則
- 遷移層のエネルギー収支－輻射損失と熱伝導
- コロナループの尺度則
  - diagnostics via CR-model
- 自転速度と活動性
- 恒星の磁場･黒点
- 活動周期

恒星と活動～彩層･コロナ～

Linsky, SP, 1985, 100, 333

恒星の磁気活動

(i)コロナからのX線

(ii)コロナからのマイクロ波

(iii)彩層～コロナからの紫外線

(iv)恒星磁場

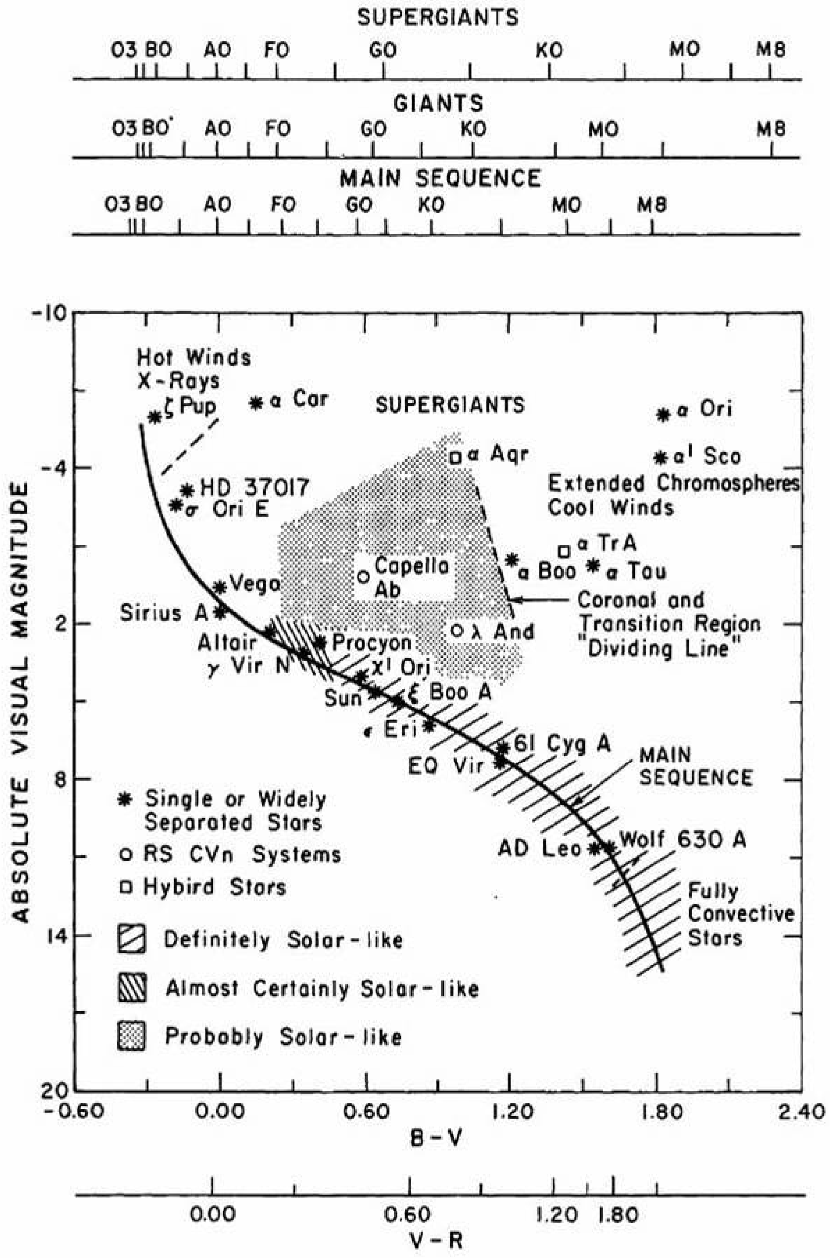

恒星と活動～彩層･コロナ～

Chromospheric Activity measured by MgII h+k lines

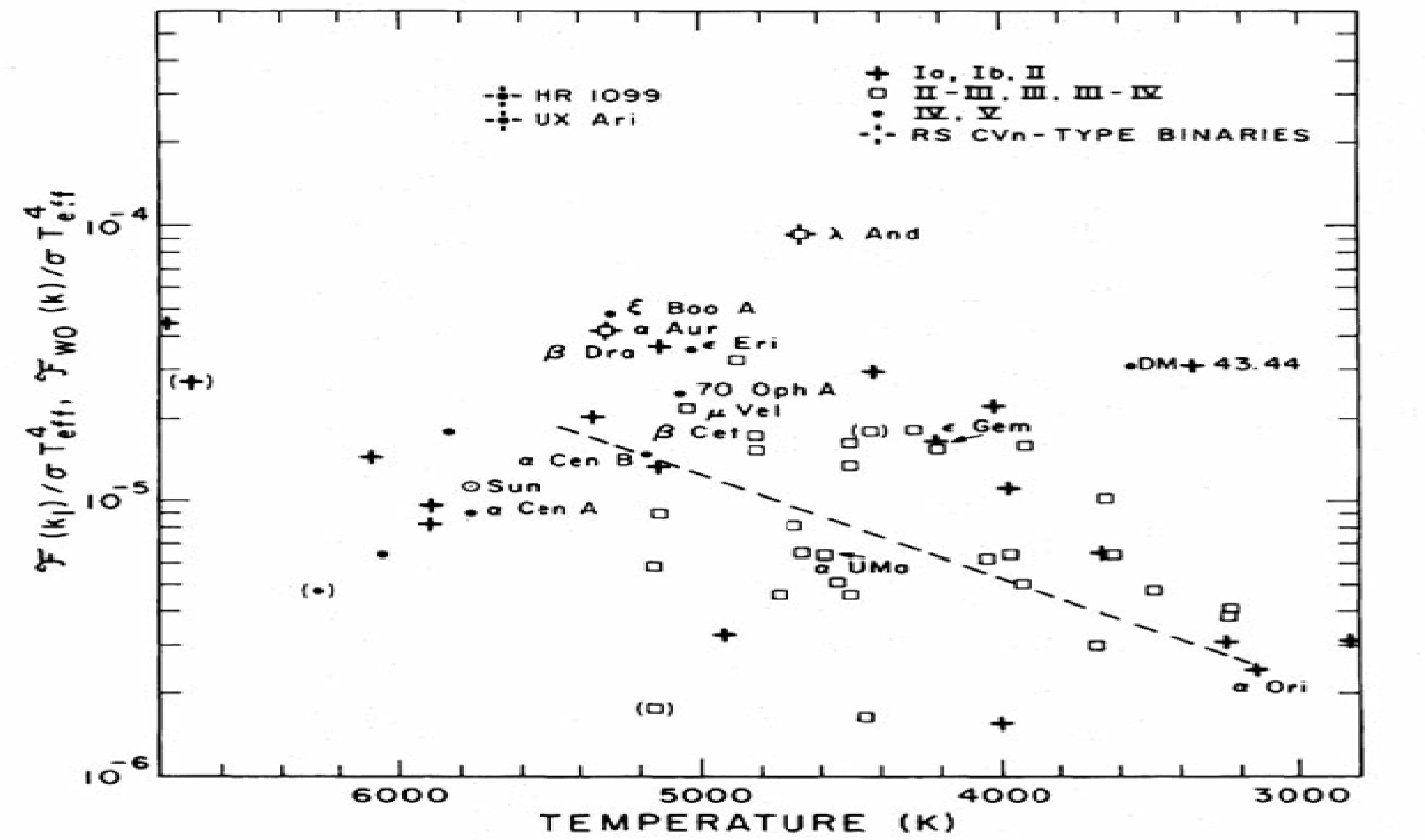

恒星と活動～彩層･コロナ～

Correlation:

Chromosphere

vs

corona

Ayres et al., 1981,
ApJ, 247, 545.

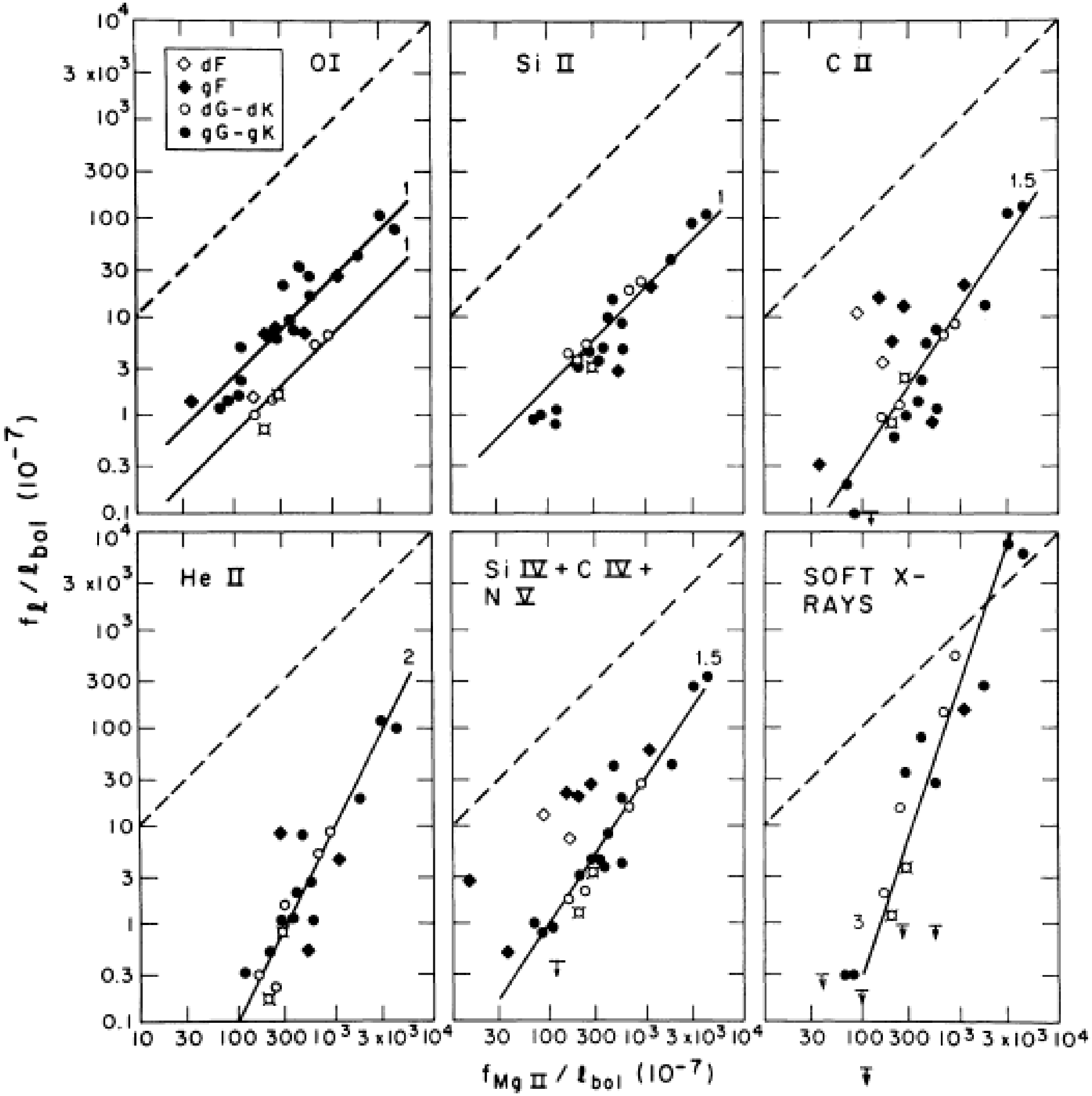

恒星と活動～彩層・コロナ～

彩層

恒星と活動～彩層･コロナ～

Energy Flux out of Stars

$$\nabla(\vec{F}_r + \vec{F}_c + \vec{F}_m + \vec{F}_g + \vec{F}_k + \vec{F}_e) = 0$$

$\vec{F}_r$; radiative $\vec{F}_c$; conductive $\vec{F}_m$; mechanical

$\vec{F}_g$; gravitational $\vec{F}_\mathrm{k}$; kinematic $\vec{F}_e$; enthalpy

at $\tau_c \sim 10^{-4}$ (T_{min}), $\Delta T \sim$ 150K

$\Delta H/H \sim 16T^3/T_{eff}^4 \Delta T \tau_c \sim 1.5 \times 10^{-5}$

Chromosphere; (3–6) $\times 10^6$ erg/cm^{2}sec

→ $\Delta H/H \sim (5\text{–}8) \times 10^{-5}$ erg/cm^{2}sec

恒星と活動～彩層･コロナ～

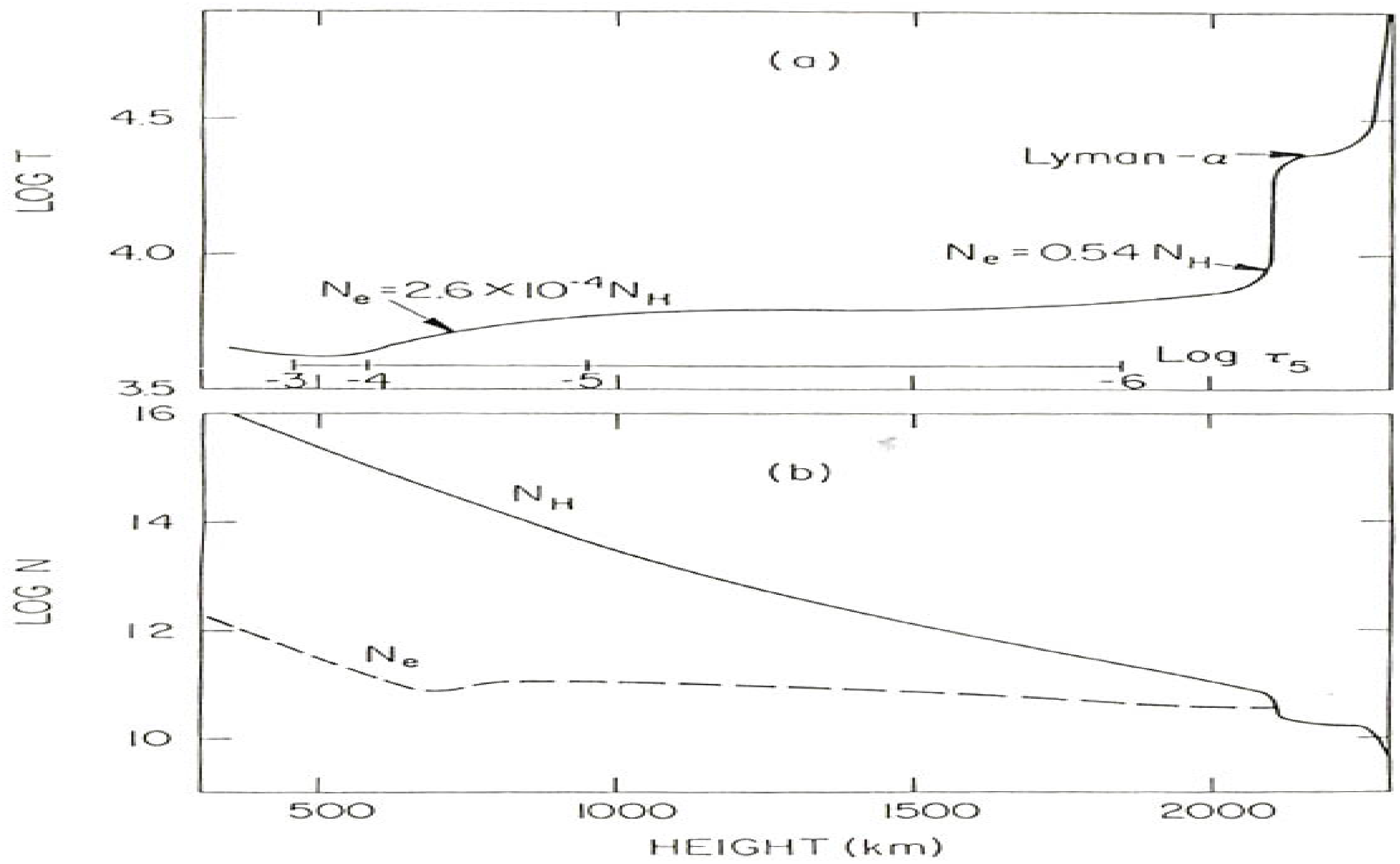

(a)
4.5
4.0
3.5
LOG T
Lyman-α
Ne=0.54 NH
Ne=2.6×10⁻⁴NH
Log τ5
-3
-4
-5
-6
(b)
16
14
12
10
LOG N
NH
Ne
500
1000
1500
2000
HEIGHT (km)

恒星と活動～彩層･コロナ～

水素の電離　electron donner at T_{min} ～metal

at T_{top}～hydrogen

Radiative loss

$$4\pi \frac{dH}{dz} = QA_{el}N_e N_H f(\tau) g(\tau)$$

Q : collision strength　　A_{el} : element abundance

$f(\tau) \sim \exp(-X_u / kT)$ collisional excitation

$g(\tau) \sim \exp(\pm A / kT)$ lower level population

恒星と活動～彩層･コロナ～

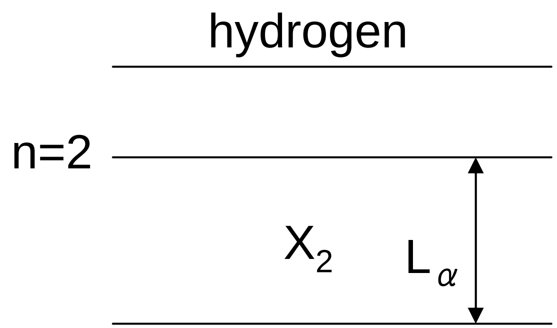

$$L = \frac{dH}{dz};\quad \text{energy loss rate /cm}^3$$

$$\frac{d\ln T}{dz} = \frac{kT}{X_u \pm A}\left(\frac{d\ln L}{dz} - 2\frac{d\ln N_H}{dz}\right) \quad N_p << N_e$$

$$= \frac{kT}{X_2 + (1+\alpha)(X_u \pm A)} \times \qquad N_p \sim N_e$$

$$\left[(1+\alpha)\frac{d\ln L}{dz} - (2+\alpha)\frac{d\ln N_H}{dz} - \frac{d\ln(1-\gamma)}{dz}\right]$$

$$\gamma = N_p/(N_p + N_{HI}) \quad X_2 : \text{n} = 2\ \text{excitation energy}$$

$$\alpha = 1\ (\tau_{LC} >> 1) \rightarrow 0\ (\tau_{LC} < 1)$$

$$N_{HI} \sim n_p n_e^{\alpha} \cdot e^{\frac{X_2}{kT}}$$

恒星と活動～彩層・コロナ～

(i) Ne ← metal

(ii) Ne ~ Np γ <<1

(iii) Ne ~ Np γ ~ 1

- $X_u \pm A \ll X_2$ → (ii) dln T/dz ~ minimum
- γ ~ 1 temperature gradient max

恒星と活動～彩層・コロナ～

Empirical Chromospheric Model

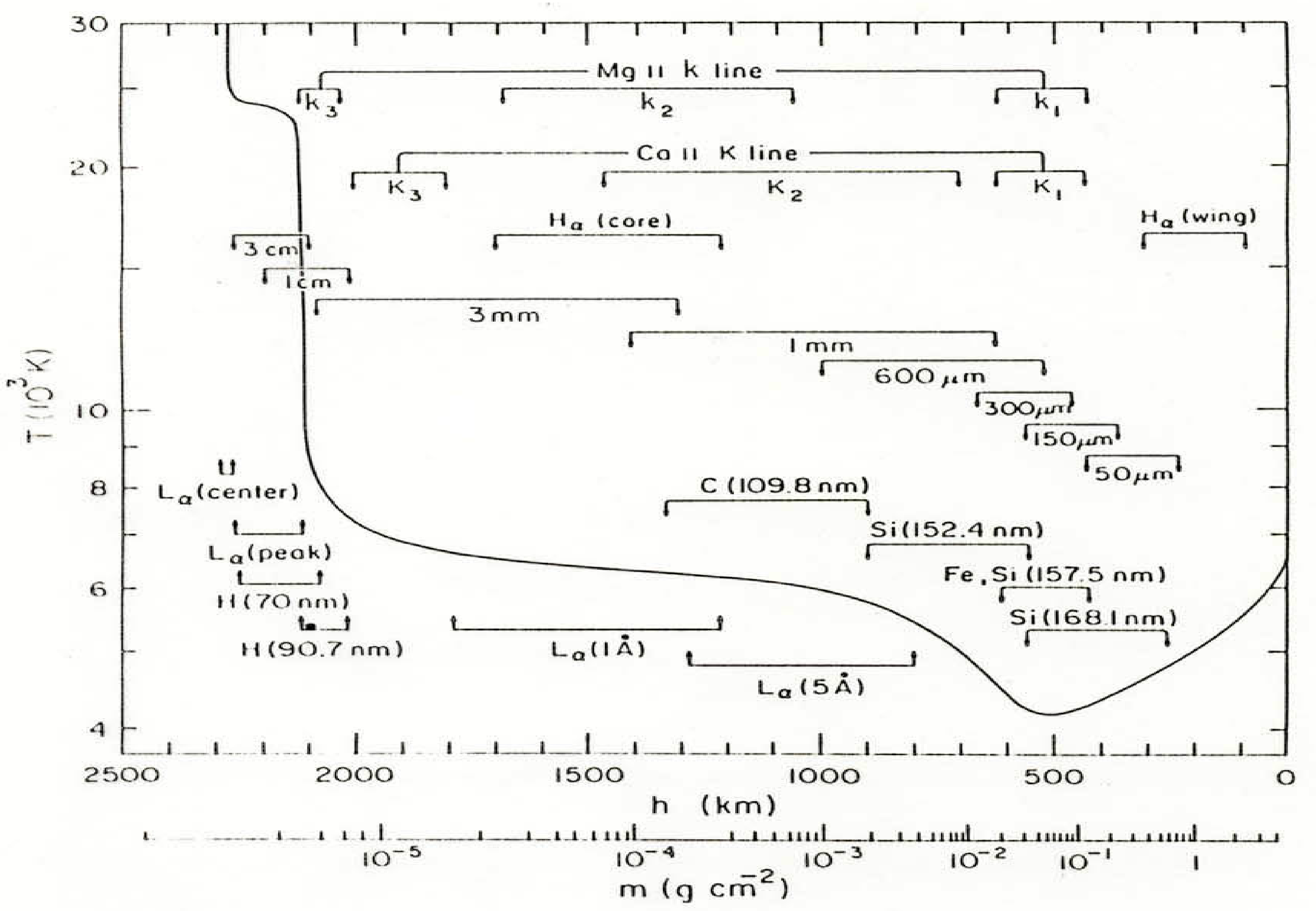

Vernazza, Avrett, Loeser: 1981, ApJS, 45, 635.

恒星と活動～彩層･コロナ～

A: dark point within a cell B: average cell center C: average quiet sun

D average network E: bright network F: very bright network element

F’: flare (Fontenla et al. 1990)….

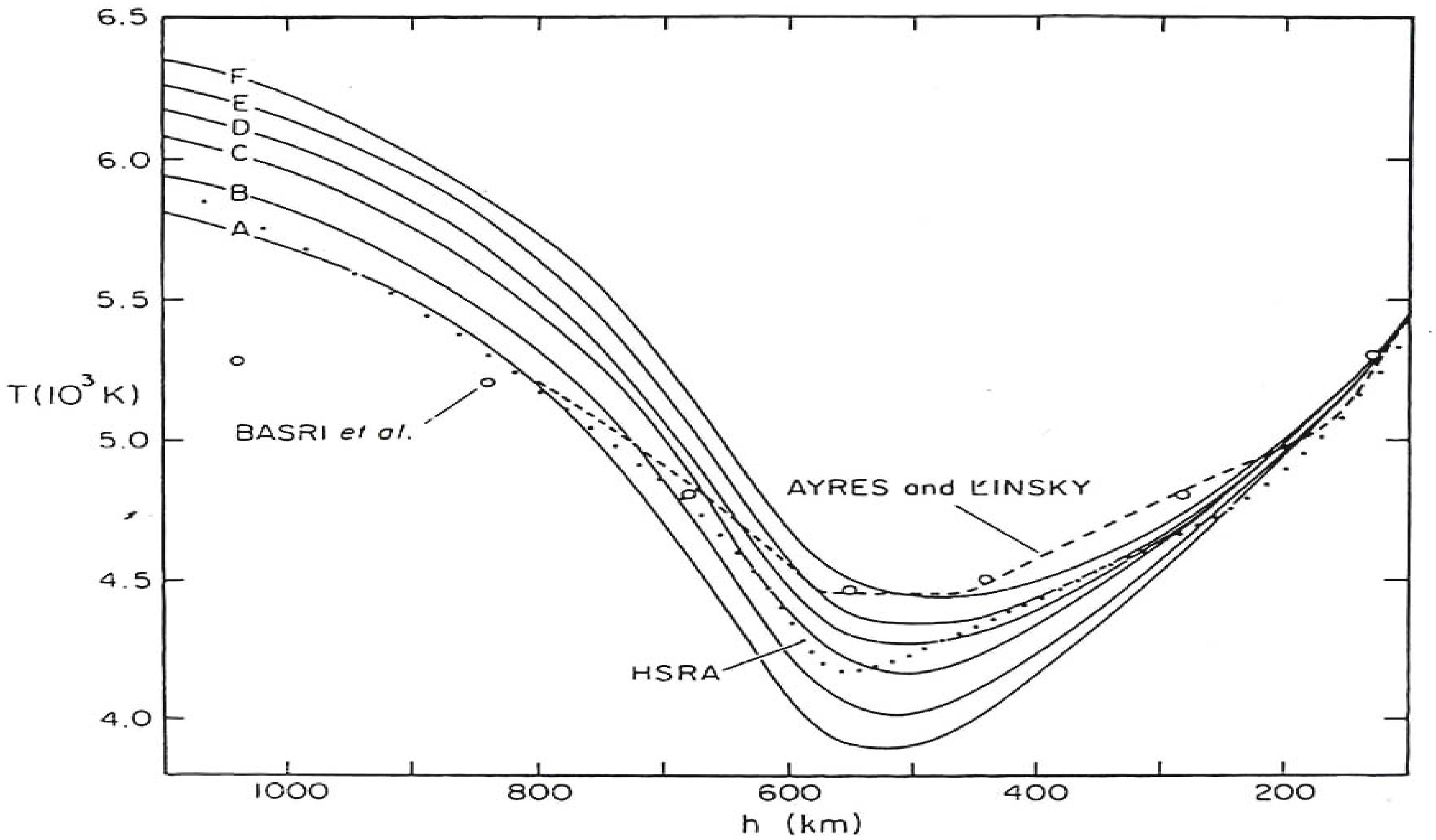

恒星と活動～彩層･コロナ～

Thermal Bifurcation (Ayres 1981, ApJ 224,1064.)

coolant CO & heater/coolant H^-

$F = e_{co} + e_{H^-}$ (=0; radiative equilibrium)

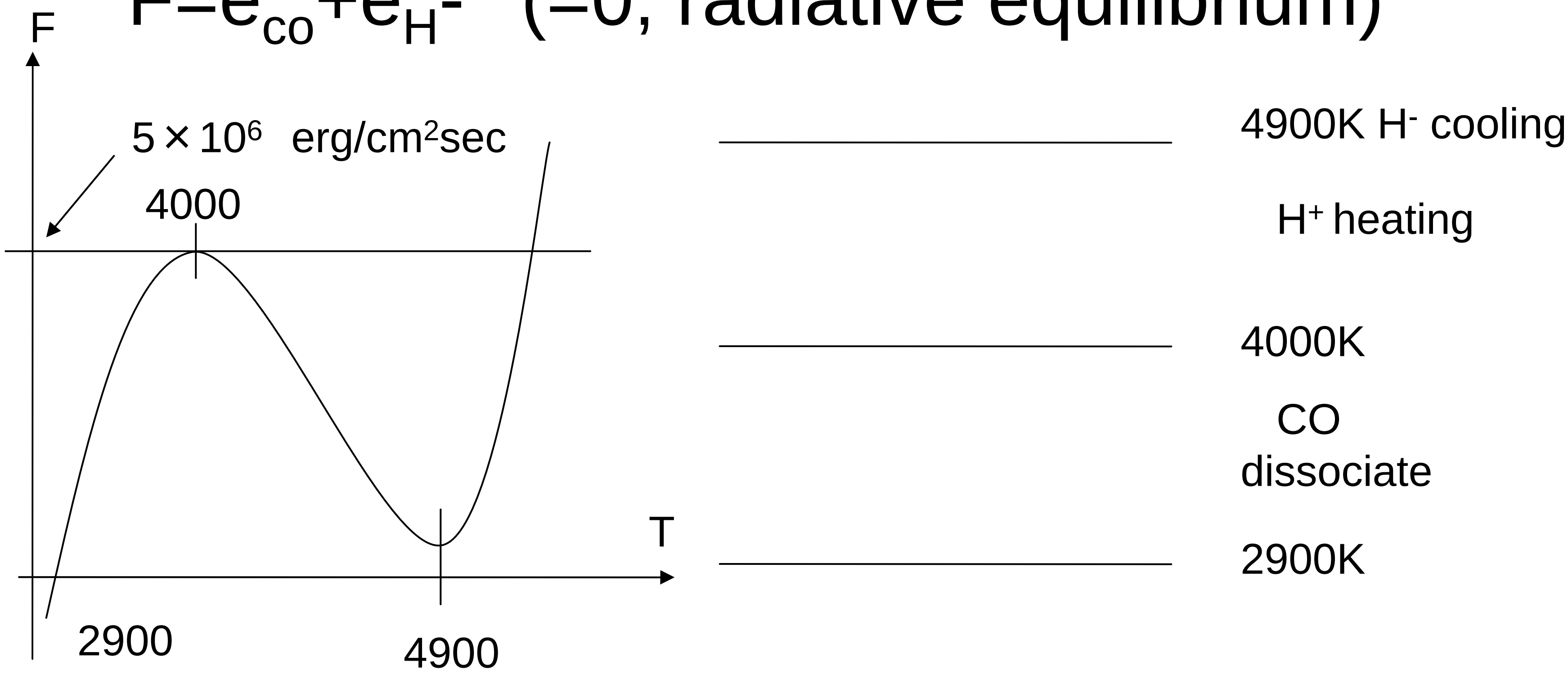

恒星と活動～彩層・コロナ～

Two-level atom without continuum

radiative transfer

$$\mu \frac{dI_\nu}{dz} = \left[-n_l B_{lu} I_\nu + n_u (A_{ul} + B_{ul} I_\nu) \right] \phi_\nu \frac{h\nu}{4\pi}$$

$$S_\nu = \frac{n_u A_{ul}}{n_u B_{ul} - n_l B_{lu}} = \frac{2h\nu^3}{c^2} \left[\left(\frac{n_l g_u}{n_u g_l} \right) - 1 \right]^{-1}$$

statistical equilibrium

$$n_l \left(B_{lu} \int \phi_\nu J_\nu d\nu + C_{lu} \right) = n_u \left(A_{ul} + B_{ul} \int \phi_\nu J_\nu d\nu + C_{ul} \right)$$

恒星と活動～彩層･コロナ～

Two level atom w/o cont.

$$S_l = \frac{\left[\int \phi_\nu J_\nu d\nu + \varepsilon' B_\nu\right]}{1+\varepsilon'} \equiv (1-\varepsilon)\bar{J}_\nu + \varepsilon B_\nu$$

$$\varepsilon' \equiv \frac{C_{lu}\left(1-e^{-\frac{h\nu}{kT}}\right)}{A_{ul}}, \qquad \varepsilon \equiv \frac{\varepsilon'}{1+\varepsilon'}$$

恒星と活動～彩層･コロナ～

等温でも吸収線ができる！

B_ν, ε ; const case → S

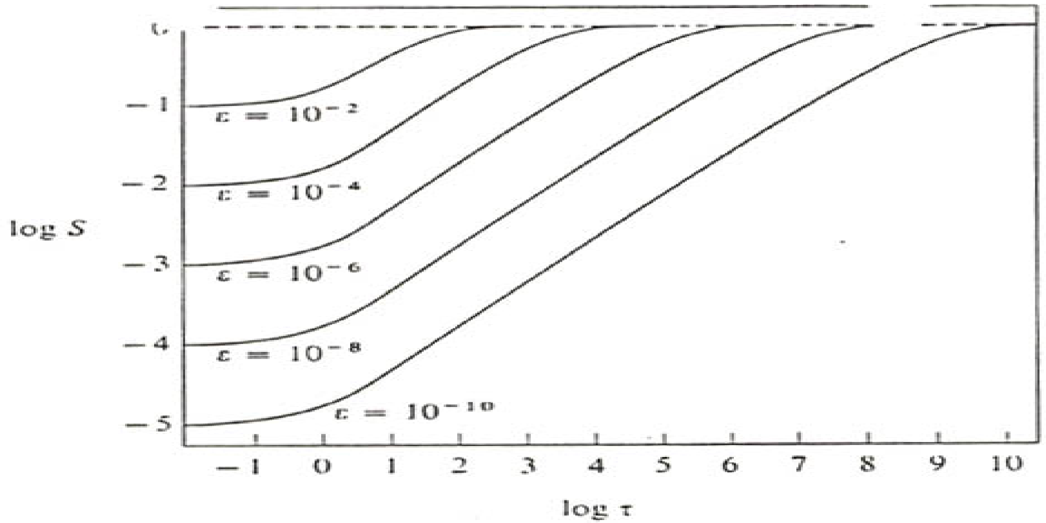

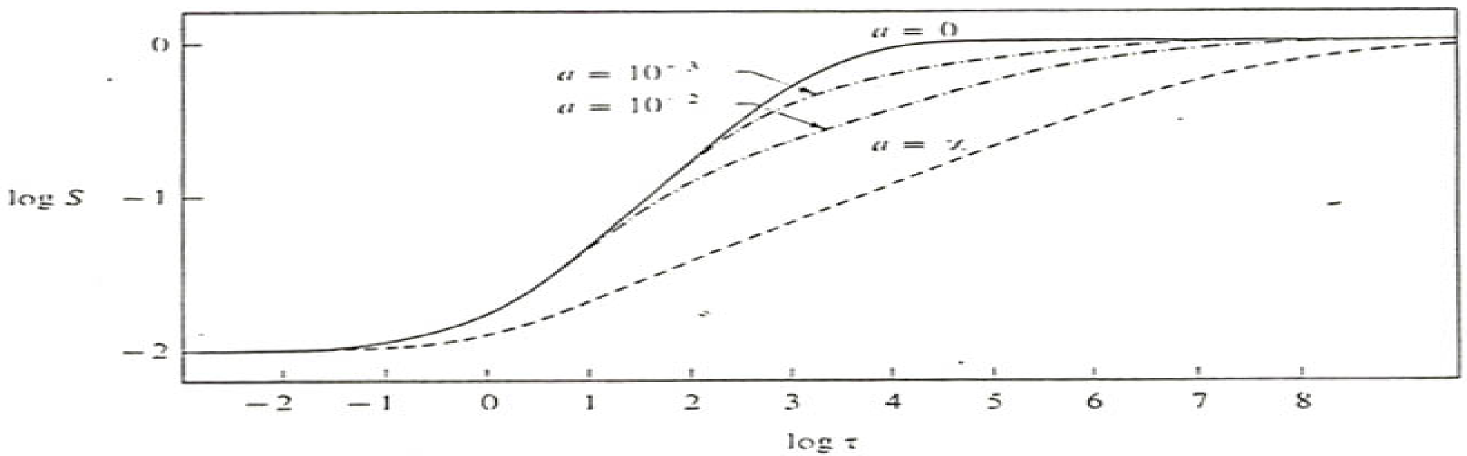

恒星と活動～彩層・コロナ～

mean free path; l_ν

photon destruction probability; P_d

thermalization depth; Λ

photon escape probability; P_e

$$l_\nu \sim \frac{1}{\chi_\nu} = \frac{1}{\chi_{lu}\phi_\nu + \chi_c}$$

$$P_d \sim \frac{C_{ul}}{C_{ul} + A_{ul}}$$

$$\Lambda; \quad P_e(\tau) = P_d(\tau)$$

$$P_e(\tau) = \int_{x_1}^{\infty} \phi(x)\,dx$$

$$\text{for } x_1; \tau_x = 1$$

恒星と活動～彩層･コロナ～

line profile ϕ(x) → thermalization depth Λ

$$\text{Doppler; } \phi(x) = \frac{1}{\pi} e^{-x^2} \qquad \Lambda \sim \frac{1}{\varepsilon}$$

$$\text{Voigt; } \phi(x) = \frac{a}{\pi\sqrt{\pi}} \int_{-\infty}^{\infty} e^{-y^2} \left[(x-y)^2 + a^2 \right]^{-1} dy \qquad \Lambda \sim \frac{a}{\varepsilon^2}$$

$$\text{Lorentz; } \phi(x) = \frac{1}{\pi} \frac{1}{x^2+1} \qquad \Lambda \sim \frac{1}{\varepsilon^2}$$

source function at the surface

$$S_l(0) = \sqrt{\varepsilon} B$$

恒星と活動～彩層･コロナ～

Wilson-Bappu Effect

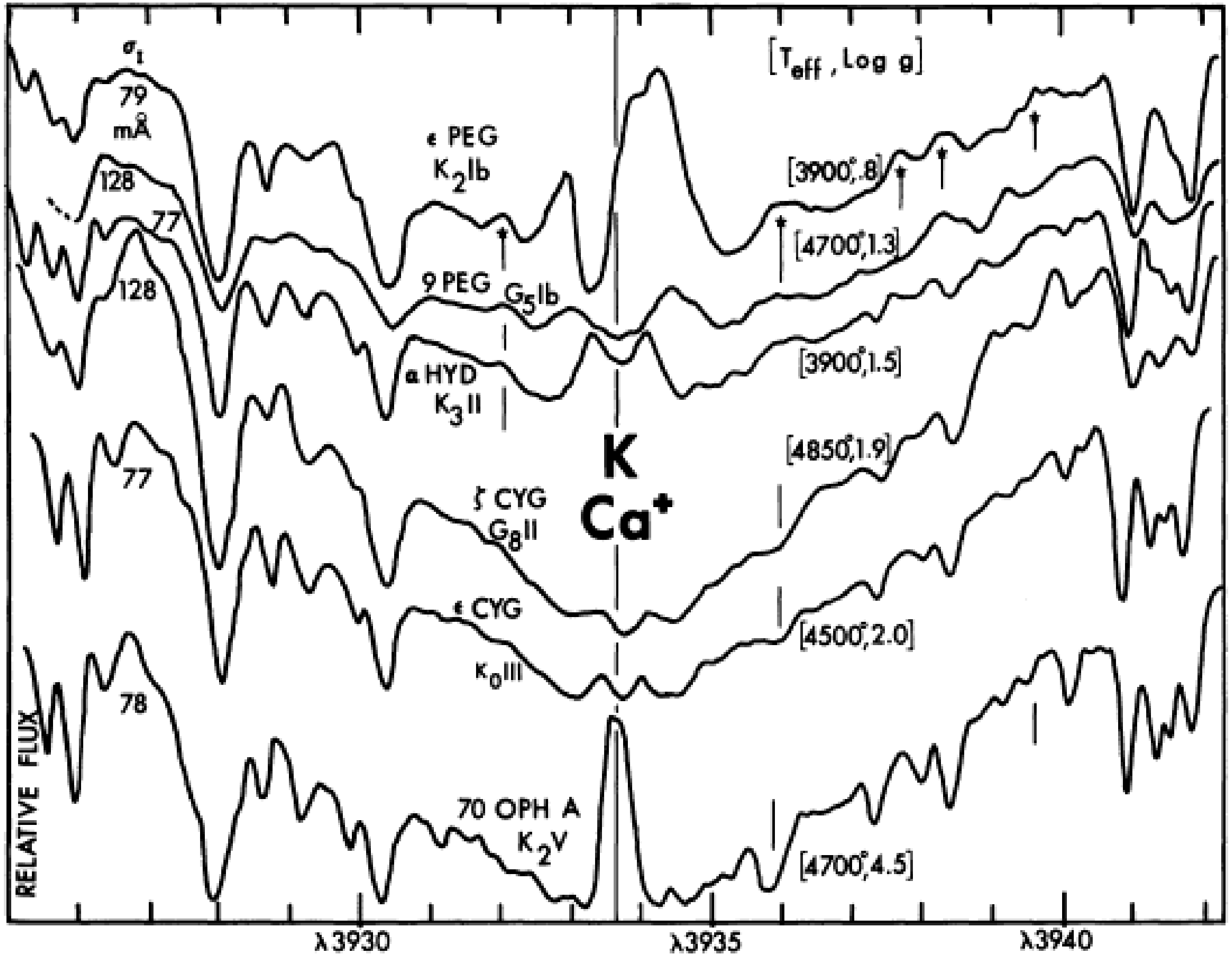

恒星と活動～彩層･コロナ～

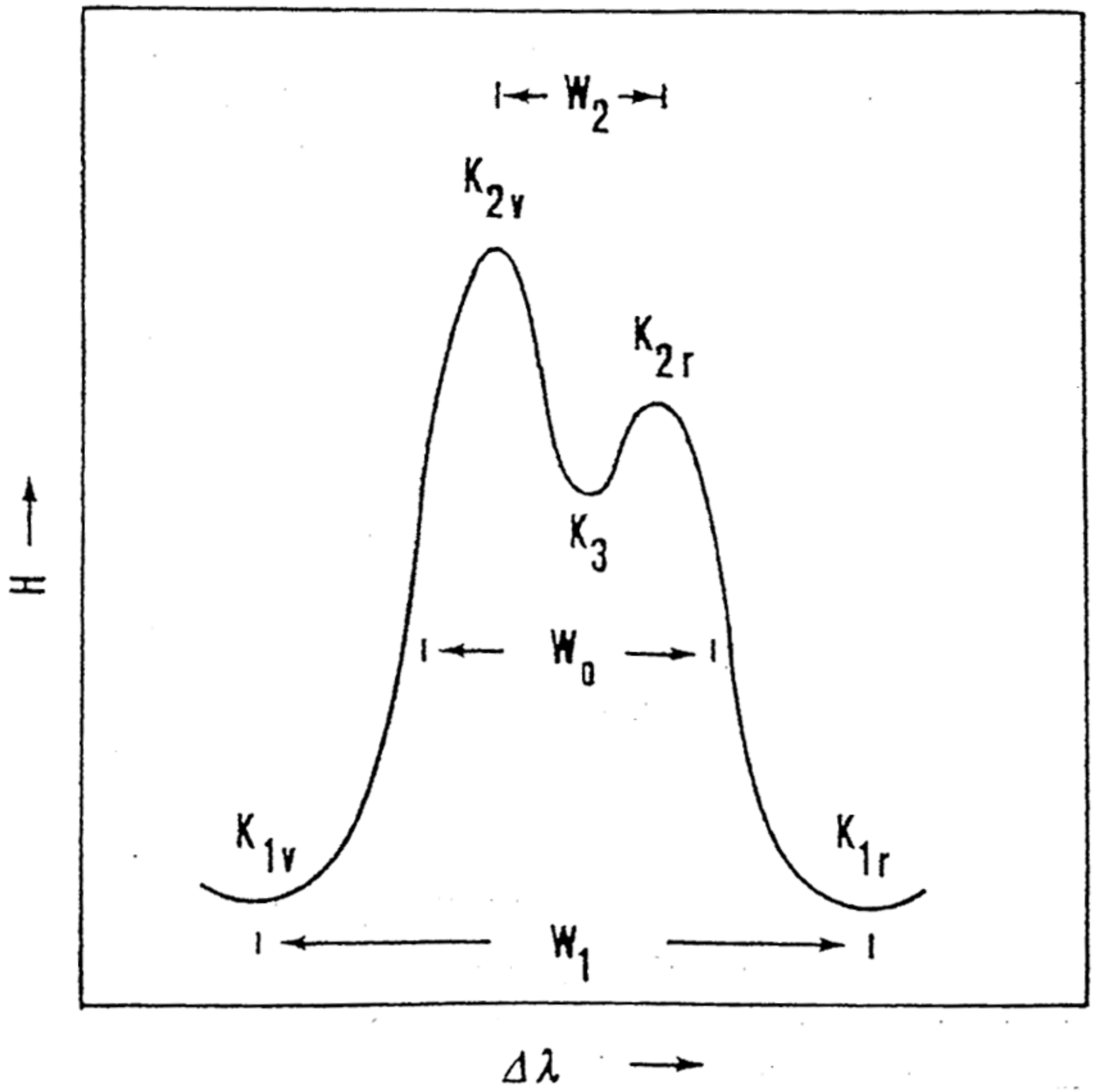

恒星と活動～彩層･コロナ～

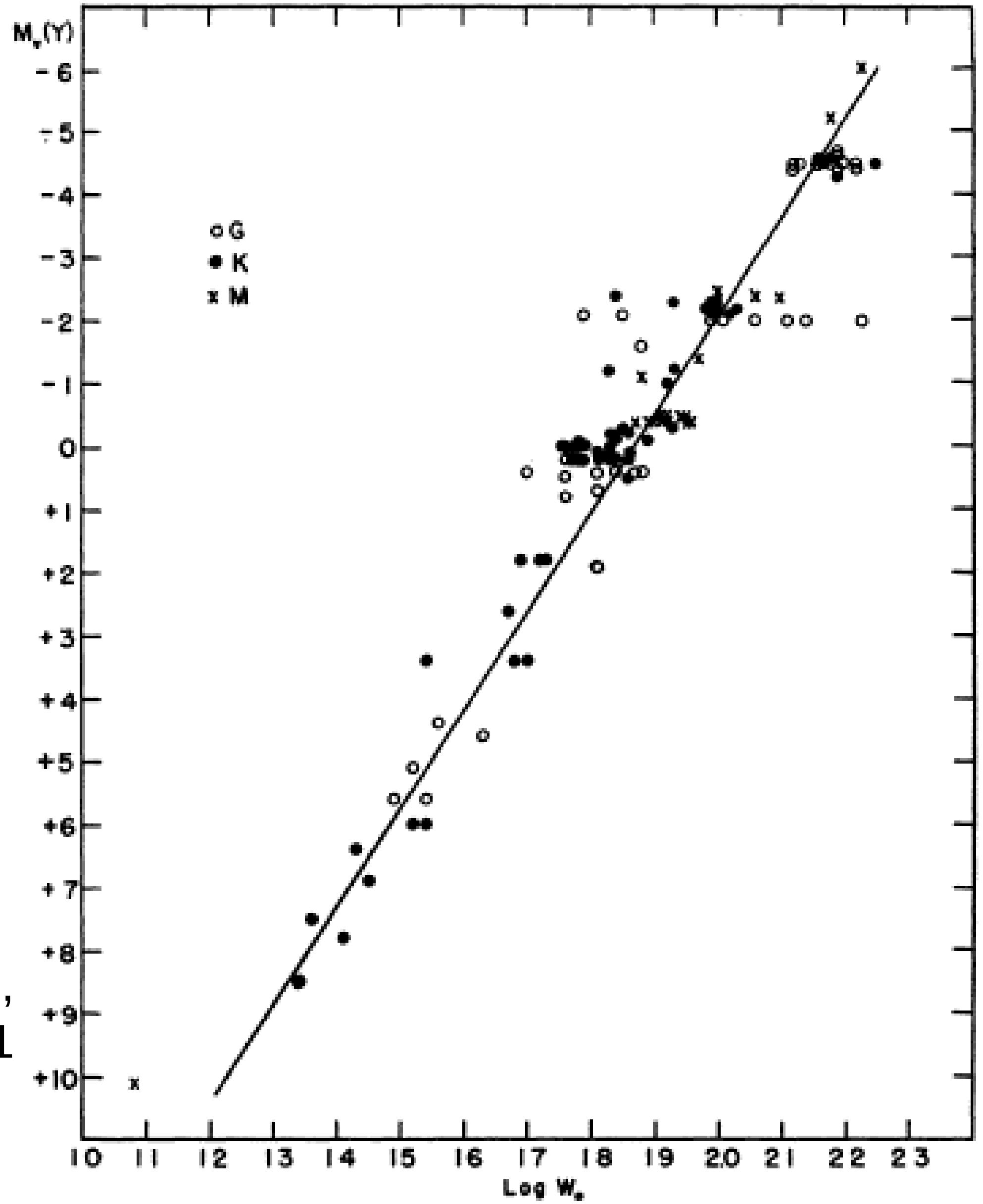

Wilson & Bappu 1957, ApJ. 125, 661

恒星と活動～彩層･コロナ～

CaIIH&K Line Formation

strong gfN-value
collision dominant
($S_\nu \approx B_\nu$ to middle chromosphere)

K_2; formed at the thermalization depth

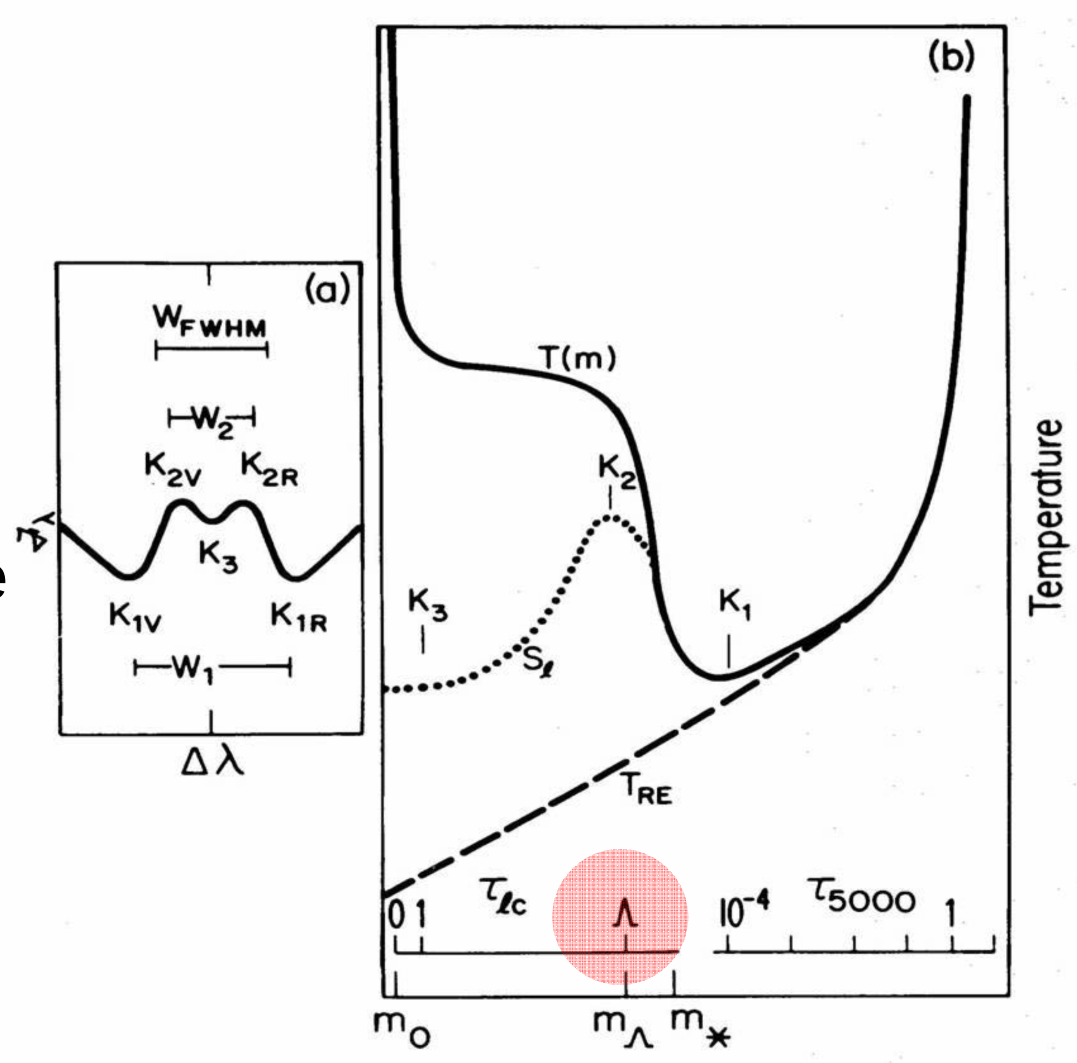

Ayres (1979)

恒星と活動～彩層・コロナ～

Wilson-Bappu Effect; Interpretation

- Chromospheric Thickness
- W_0; Dopper control?
- Inside K1, k1; optically thick in chromosphere
- ← effect of radiative transfer
- Ayres 1979, ApJ 228, 509

$$\frac{dF}{dm} \sim \frac{F^{tot}}{m_*}, \quad *: \text{temperature min.}$$

$$F^{tot} \sim F_{MgII}, \quad F_{MgII} / \sigma T_{eff}^4 \sim T_{eff}^{2\pm2}$$

$$F_{\odot}^{tot} \sim 7 \times 10^6 erg / cm^2 s$$

$$\sim 7 \times 10^6 \tilde{F} T_{eff}^{6\pm2}$$

恒星と活動～彩層・コロナ～

$$\left.\frac{dF}{dm}\right)_* \sim \left.\frac{dF}{dm}\right)_{H^-} \sim Cn_e^* \sim \frac{P^*}{T_*}\tilde{A}_{Fe}$$

$$T_* \sim 0.75T_{eff} \qquad P = mg \quad \text{(hydrostatic)}$$

経験的

$$m_* \sim \tilde{A}_{Fe}^{-1/2}\tilde{F}^{1/2}\tilde{g}^{-1/2}\tilde{T}_{eff}^{7/2\pm1}$$

Lorentzian wing control of K1

$$\tau_{\Delta\lambda_*} \sim \kappa_l \tilde{A}_{el}\, m_* \Delta\lambda_*^{-2}$$

$$\Delta\lambda_* \sim \kappa_l^{1/2}\left(\frac{\tilde{A}_{el}}{\tilde{A}_{Fe}}\right)^{-1/2}\tilde{A}_{Fe}^{1/4}\tilde{F}^{1/4}\tilde{g}^{-1/4}T_{eff}^{\frac{7}{4}\pm\frac{1}{2}}$$

$$\Delta\lambda^{k1} / \Delta\lambda^{kK1} \sim 2.5$$ （観測：太陽　～2.3）

恒星と活動～彩層･コロナ～

TABLE

Adopted Line Parameters*

Parameter	Ca II K	Mg II *k*
λ_l (Å)	3934	2796
g_2/g_1	2	2
A_{21} (s^{-1})	1.5×10^8	2.7×10^8
f†	0.70	0.63
Γ_R (rad s^{-1})	1.5×10^8	2.7×10^8
$A_{el}^{\odot}$ ($A_H = 1.0$)	2×10^{-6}	3×10^{-5}
κ_l ($cm^2\ g^{-1}$ Å^2)‡	1.6	9.8
κ_{lc} [$cm^2\ g^{-1}\ (km\ s)^{-1}$]§	3.6×10^6	3.4×10^7
Ω_{12} ($cm^3\ s^{-1}$)	5.8×10^{-7}	7.3×10^{-7}
ϵ_l (cm^3)‖	1.9×10^{-15}	1.4×10^{-15}

* From Shine 1973, Appendix A, unless otherwise indicated.

† $f = 1.5 \times 10^{-16} \lambda_{Å}^2 (g_2/g_1) A_{21}$ (Allen 1973, p. 59).

‡ $\kappa_l \equiv (\pi e^2/m_e c) f (\lambda_l^4/c^2)(\Gamma_R/4\pi^2)(A_{el}^{\odot}/1.4 m_H)$.

§ $\kappa_{lc} \equiv (\pi e^2/m_e c) f (\lambda_l/\sqrt{\pi})(A_{el}^{\odot}/1.4 m_H)$.

‖ $\epsilon_l \equiv \Omega_{21}/A_{21} = [(g_1/g_2)\Omega_{12}/A_{21}]$.

恒星と活動～彩層･コロナ～

$$\Lambda \sim \frac{1}{\varepsilon}$$ (thermalization length)

$$\tau_{lc} \approx \kappa_{lc} \tilde{A}_{el} \xi^{-1} m_{\Lambda} = \Lambda \sim (\varepsilon_l n_l)^{-1}$$

$$\varepsilon_l \equiv \Omega_{ul} / A_{ul}$$ ξ: Doppler velocity

$$n_l \sim \tilde{F} \tilde{T}_{eff}^{6\pm 2} m_*^{-1} \sim \tilde{A}_{Fe}^{-1/2} \tilde{F}^{1/2} \tilde{g}^{1/2} \tilde{T}_{eff}^{5/2\pm 1}$$

$$n_l \sim \overline{\frac{dF}{dm}} \sim \frac{F^{tot}}{m_*}$$ chromosphere mean density

$$m_{\Lambda} \sim \kappa_{lc}^{-1} \varepsilon_l^{-1} \left(\frac{\tilde{A}_{el}}{\tilde{A}_{Fe}} \right)^{-1} \tilde{A}_{Fe}^{2/3} \tilde{F}^{-1/2} g^{-1/2} T_{eff}^{-(\frac{5}{2}\pm 1)} \xi$$

$$\Delta\lambda_{\Lambda}^{k} / \Delta\lambda_{\Lambda}^{K} \sim 0.9$$ (観測:太陽 ~1)

恒星と活動～彩層･コロナ～

- W(K1), W(K2) とも$g^{-1/4}$でスケールする
- W(K2)~$\xi^{1/2}$ でスケールする
- W(K2) ↑　F↓,　while W(K1)↑　F↑

←観測 ○solar plage

恒星と活動～彩層･コロナ～

遷移層･コロナ

恒星と活動～彩層･コロナ～

遷移層のエネルギー収支－輻射損失と熱伝導

(corona) $H_c = R_c + C_c$

(transition region) $H_{tr} + C_c = R_{tr}$

Observation: $R_{tr} \sim C_c \rightarrow \underline{H_{tr} \sim 0}$

恒星と活動～彩層･コロナ～

CR Modelling under coronal condition

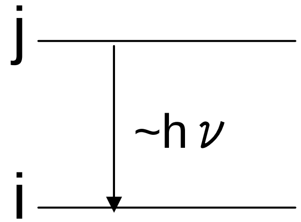

- Line intensity of a permitted line (j → i)

$$\varepsilon(\lambda_{ij}) = \frac{hc}{\lambda_{ij}} A_{ji} N_j$$ (Emissivity /volume)

$$N_j = \frac{N_j(X^{+m})}{N(X^{+m})} \frac{N(X^{+m})}{N(X)} \frac{N(X)}{N(H)} \frac{N(H)}{N_e} N_e$$

$$A_{ji} N_j = N_e C_{ij} N(X^{+m})$$ ←radiative-collisional model

$$\varepsilon(\lambda_{ij}) = \frac{hc}{\lambda_{ij}} C_{ij} N_e N(X^{+m})$$ excited state << ground state

$$C_{ij} = 8.63 \times 10^{-6} T_e^{-\frac{1}{2}} \frac{\Omega_{ij}}{\omega_i} \pi a_0^2 \exp(-\frac{\Delta E_{ij}}{kT_e})$$

恒星と活動～彩層・コロナ～

$$\varepsilon_{ij} = \beta G(T) N_e^2$$

↓ element abundance

$$\beta = 8.63 \times 10^{-6} \frac{hc}{\lambda_{ij}} \frac{\Omega_{ij}}{\omega_i} \frac{N(X)}{N(H)} \frac{N(H)}{N_e}$$

$$G(T) = \frac{N(X^{+m})}{N(X)} \frac{\exp(-\Delta E_{ij} / kT_e)}{T_e^{1/2}}$$

↑ ion fraction

G(T); contribution function

恒星と活動～彩層･コロナ～

$$I = \beta \iiint G(T) N_e^2 dV$$

$$= \beta G(T_m) \iiint N_e^2 dV \ \text{(isothermal)}$$

$$dV = dS dh \qquad \frac{dT}{dh} \equiv \nabla T$$

$$= \beta \iiint G(T) N_e^2 \frac{1}{\nabla T} dS dT$$

← differential emission measure

恒星と活動～彩層･コロナ～

Classical transition region DEM analysis

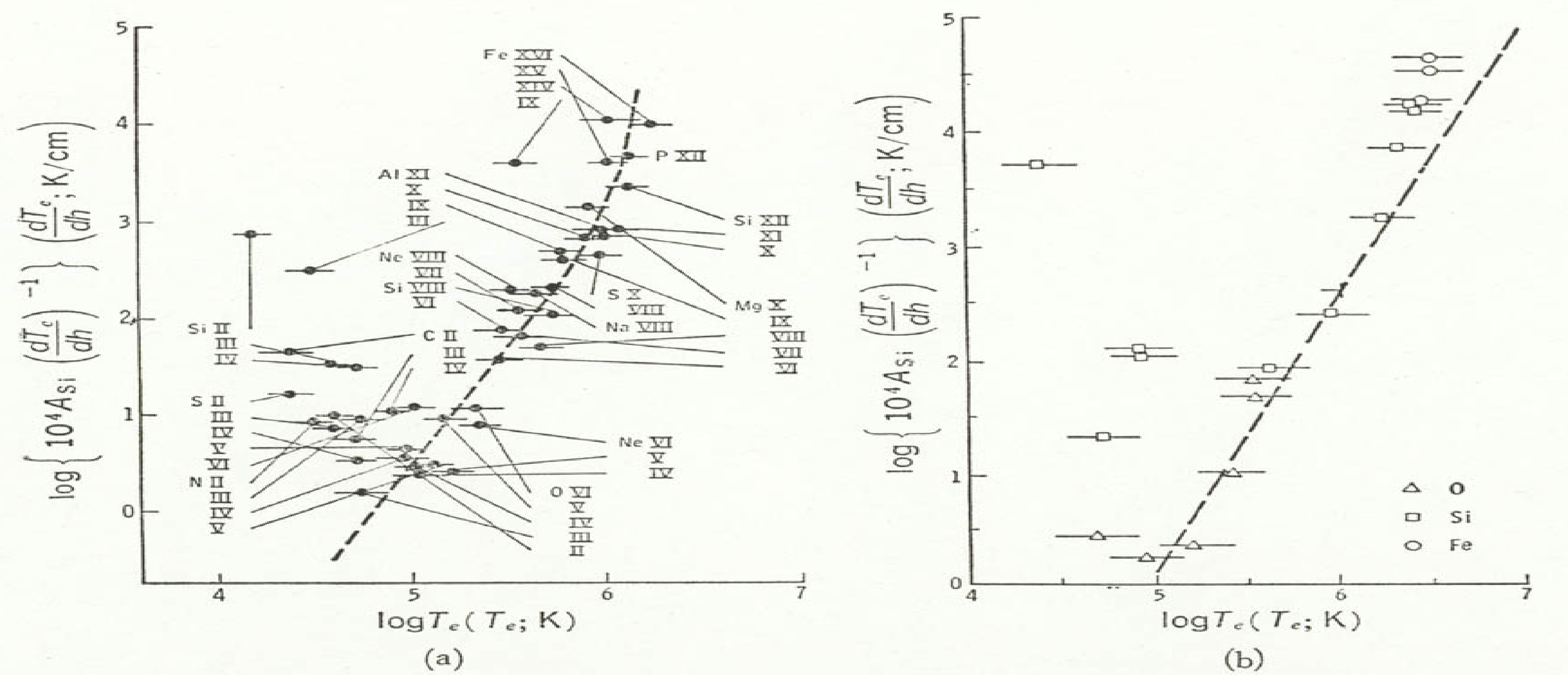

図 5－32　XUVデータから求めた遷移域における温度と温度勾配との関係　点線はデータをよく再現する線で，10^5～10^6K の範囲では熱伝導フラックスが一定（$T_e^{5/2} dT_e/dh$＝一定）なことを示す．Si の存在量を 3×10^{-5} とすると，(a)，(b)に対する F_c の値はそれぞれ，3×10^5 erg/cm² sec および 1×10^6 erg/cm² sec となる（Athay, 1971）．(a)；2電子再結合を含まない（Athay, 1966b による）．(b)；電子再結合を含む（Dupree & Goldberg, 1967 による）．

恒星と活動～彩層･コロナ～

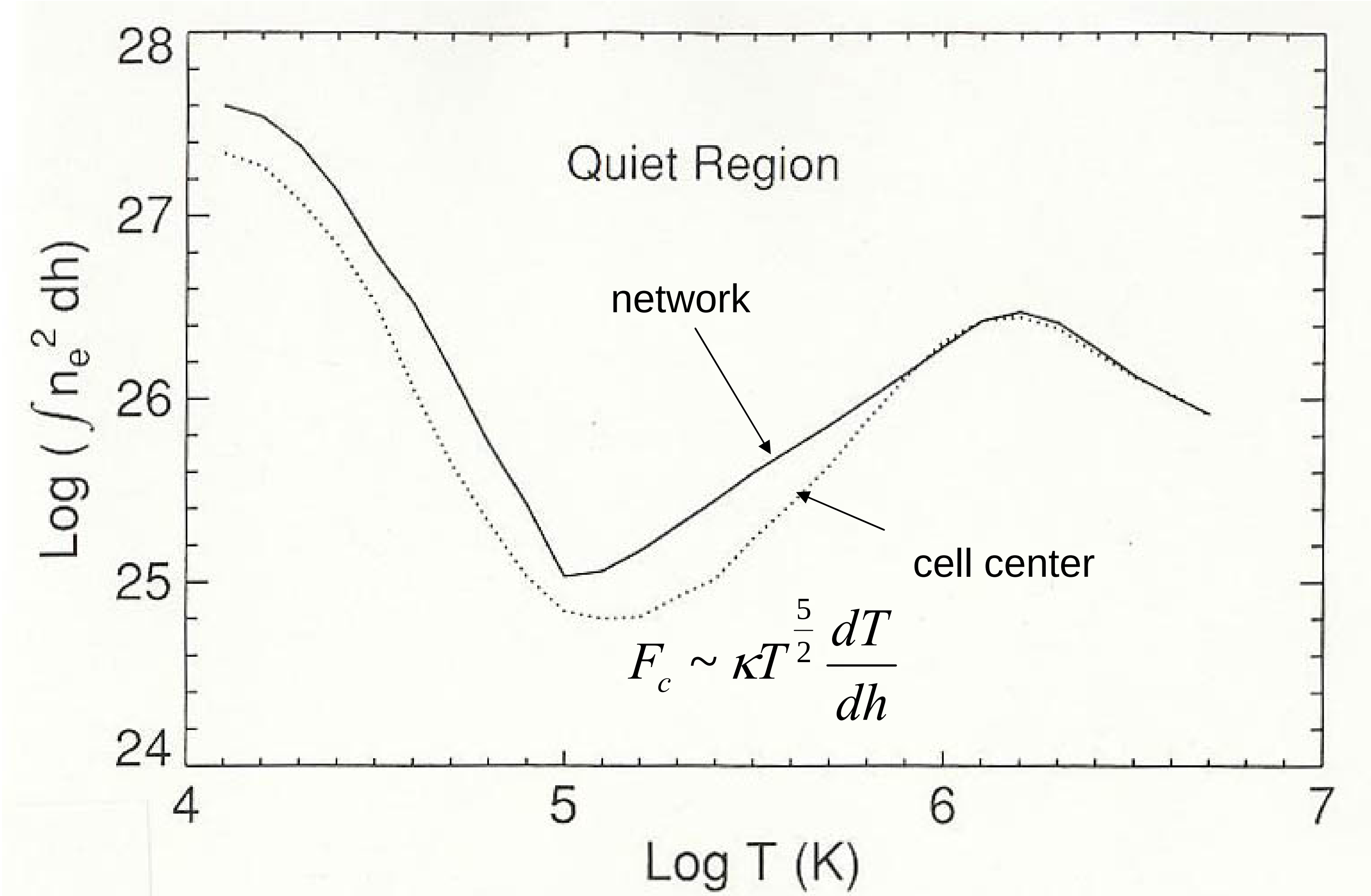

$$F_c \sim \kappa T^{\frac{5}{2}} \frac{dT}{dh}$$

恒星と活動～彩層・コロナ～

コロナの構造の多様性

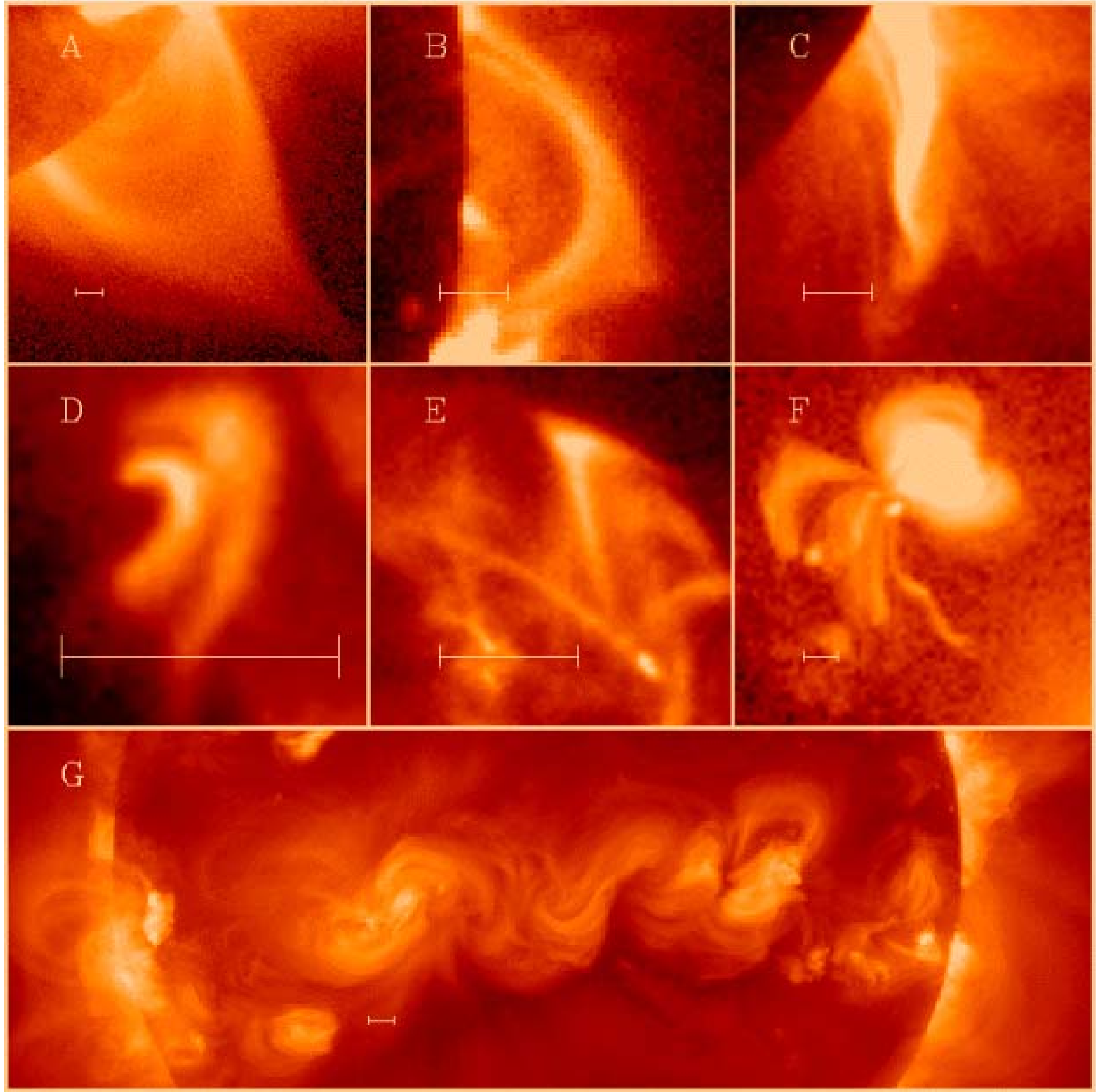

恒星と活動～彩層・コロナ～

コロナループの尺度則

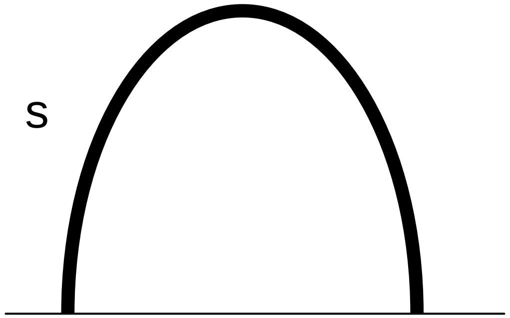

$$\frac{dF_c}{ds} = n_e^2 \chi T^{-\frac{1}{2}} - H, \quad H \sim const.(erg \cdot cm^{-3})$$

$$\chi \sim 10^{-18.81} \ (Raymond)$$

$$F_c dF_c \sim \left(\frac{p}{2k}\right)^2 \chi \kappa_0 dT - H \kappa_0 T^{\frac{5}{2}} dT, \quad F_c = \kappa_0 T^{\frac{5}{2}} \frac{dT}{ds}$$

$$\left(\frac{F_c}{2}\right)^2 \sim \left(\frac{p}{2k}\right)^2 \chi \kappa_0 (T - T_m) - \frac{7}{2} H \kappa_0 (T^{\frac{7}{2}} - T_m^{\frac{7}{2}})$$

$$T \sim 0, \quad F_c \sim 0 \ (thermally \ \ isolated) \quad \rightarrow \quad H \sim \frac{7}{2}\left(\frac{p}{2k}\right)^2 \chi T_m^{-\frac{5}{2}}$$

恒星と活動～彩層･コロナ～

$$\frac{dt}{ds} = \left(\frac{\chi}{2k^2\kappa_0}\right)^{\frac{1}{2}} \frac{p}{T_m^3} \frac{\sqrt{1-t^{\frac{5}{2}}}}{t^2} \qquad t \equiv \frac{T}{T_m}$$

$$\gamma T_m^3 \sim \left(\frac{\chi}{2k^2\kappa_0}\right)^{\frac{1}{2}} pl, \qquad \gamma \equiv \int_0^1 \frac{t^2}{\sqrt{1-t^{\frac{5}{2}}}} dt = \frac{2}{5}\sqrt{\pi}\,\Gamma\left(\frac{6}{5}\right)\Gamma\left(\frac{17}{10}\right)$$

$$f_{tot} \equiv 2\int_0^{l/2} H ds = \left(\frac{\chi\kappa_0}{2k^2}\right)^{\frac{1}{2}} p T_m^{\frac{1}{2}} \delta, \qquad \delta = \int_0^1 \frac{t^{-\frac{1}{2}}}{\sqrt{1-t^{\frac{5}{2}}}} dt$$

Rosner, Tucker, & Viana (1978)

Kano & Tsuneta (1995)

恒星と活動～彩層･コロナ～

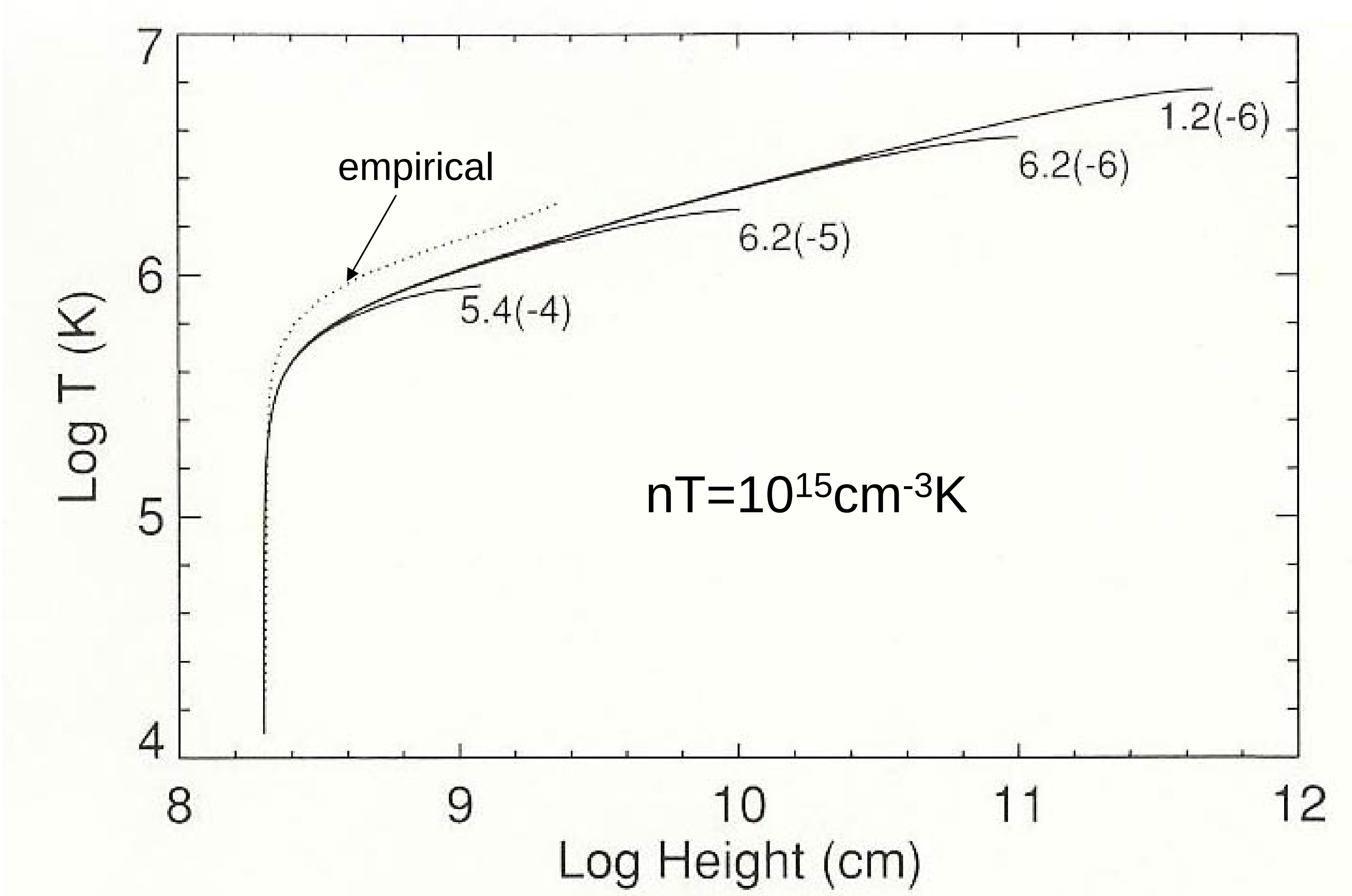

恒星と活動～彩層･コロナ～

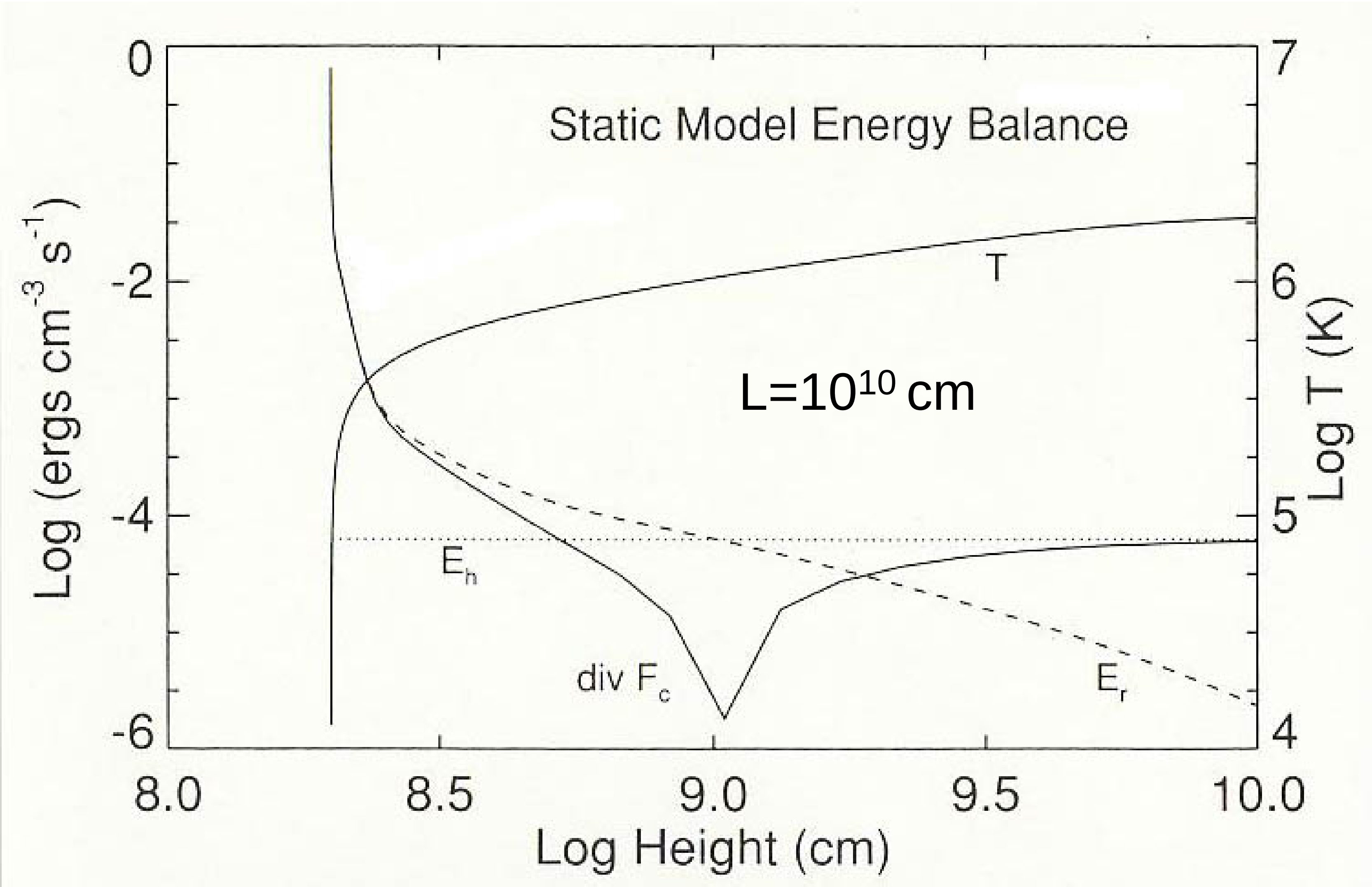

Static Model Energy Balance
T
L=10^10 cm
E_h
div F_c
E_r
0
-2
-4
-6
7
6
5
4
8.0
8.5
9.0
9.5
10.0
Log Height (cm)
Log (ergs cm^-3 s^-1)
Log T (K)

恒星と活動～彩層・コロナ～

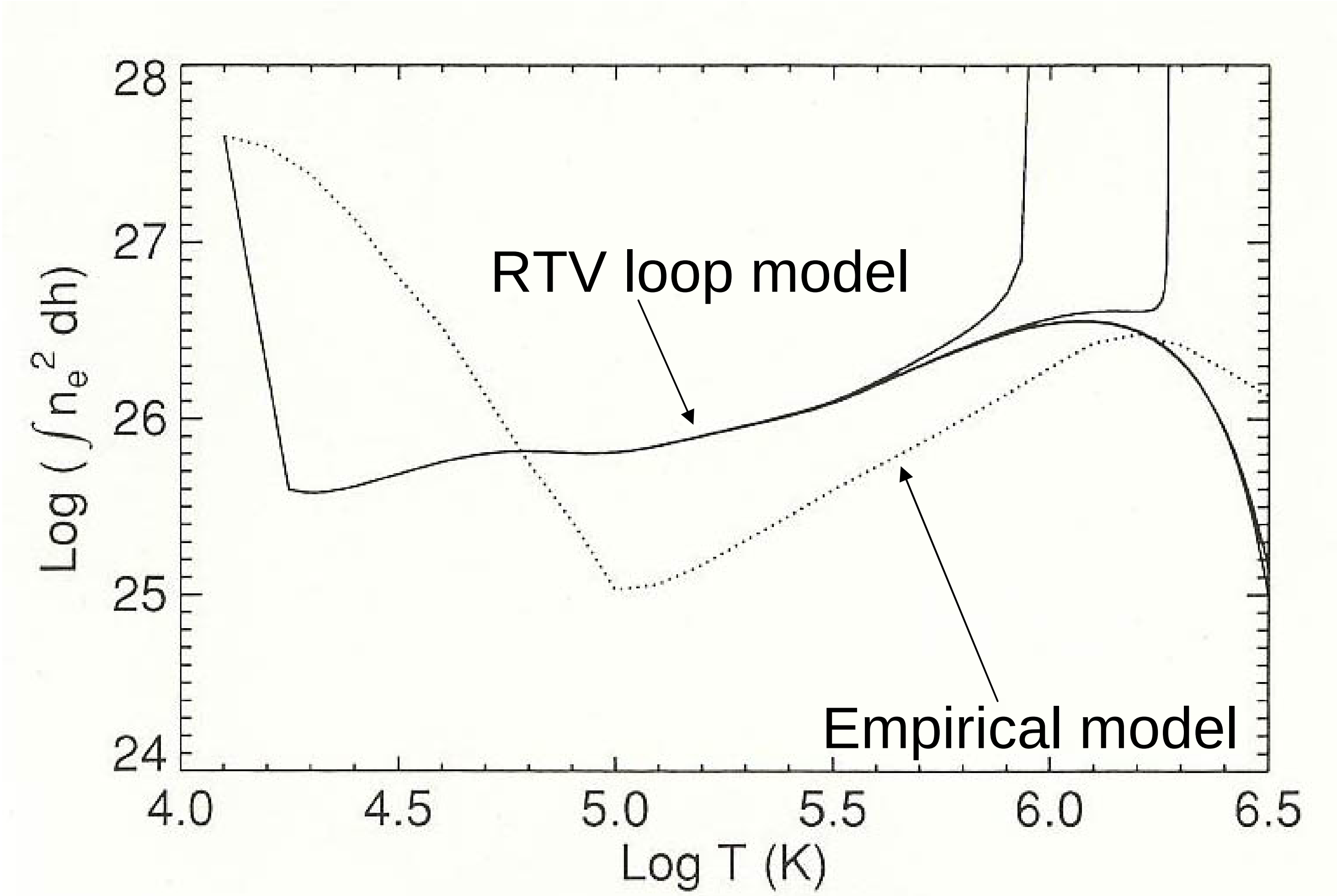
28
27
26
25
24
Log (∫ne² dh)
4.0
4.5
5.0
5.5
6.0
6.5
Log T (K)
RTV loop model
Empirical model

恒星活動

自転速度

恒星と活動～彩層･コロナ～

Chromospheric Activity measured by MgII h+k lines

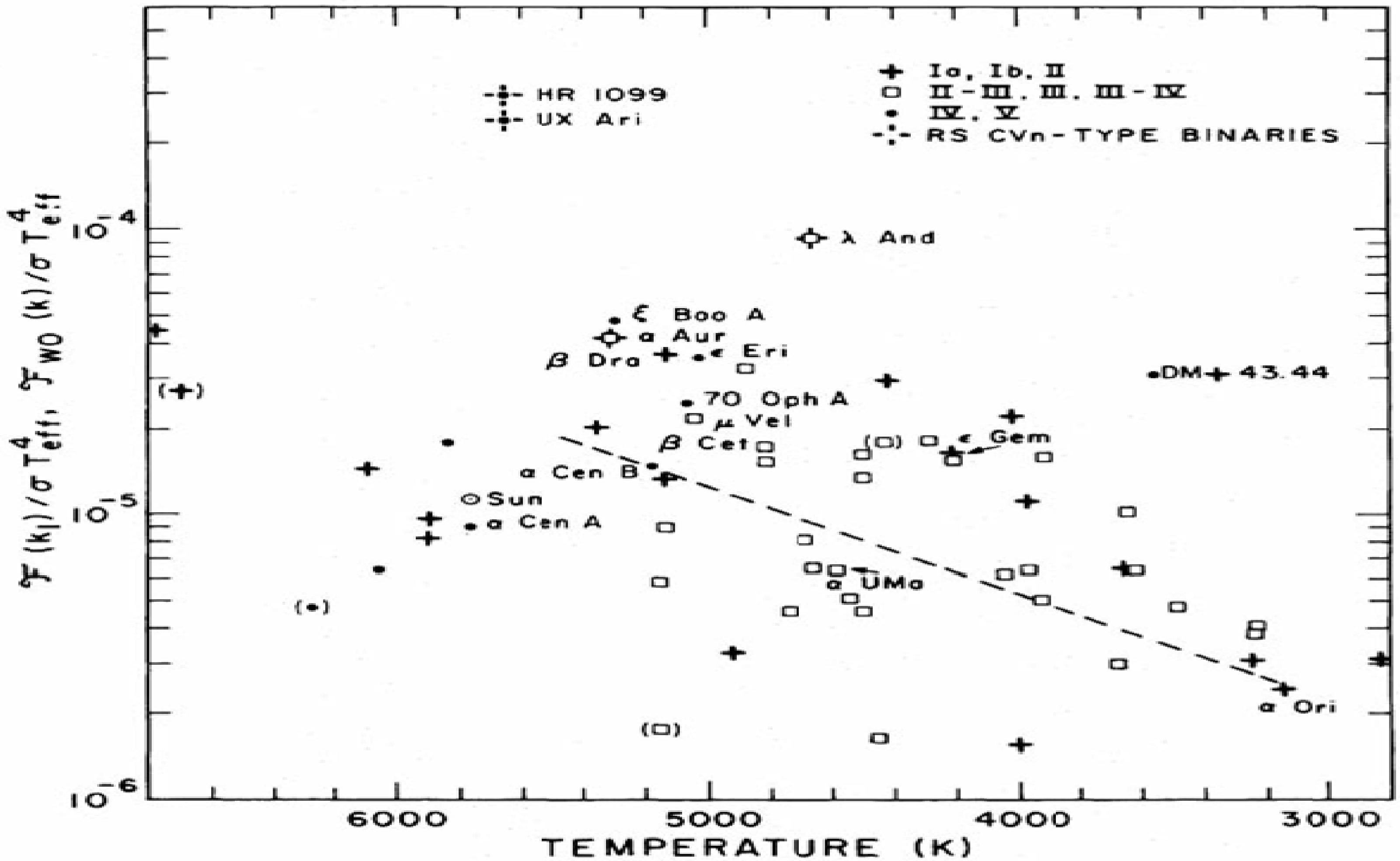

恒星と活動～彩層･コロナ～

Correlation:

Chromosphere

vs

corona

Ayres et al., 1981,
ApJ, 247, 545.

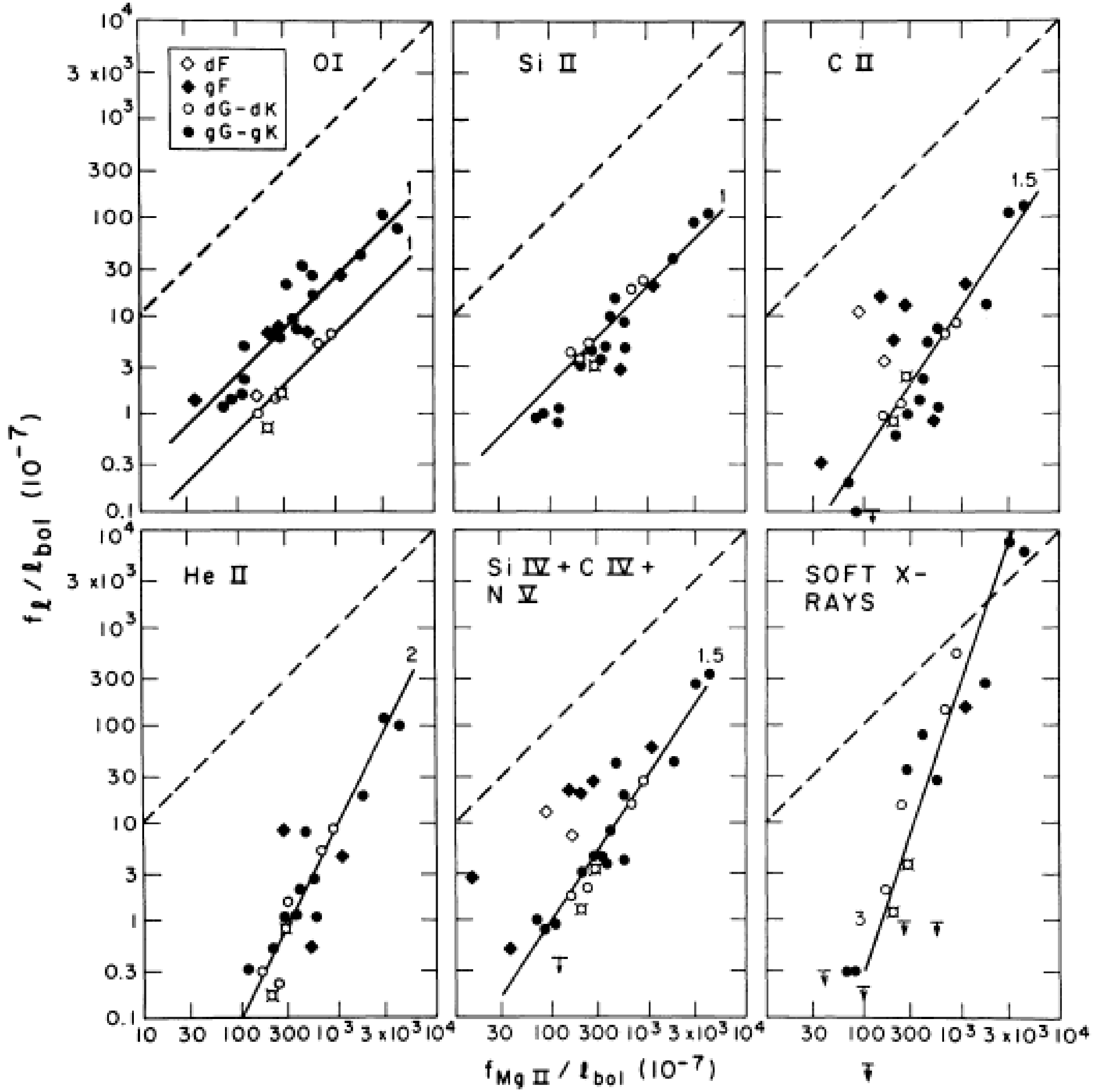

恒星と活動～彩層･コロナ～

Rotation Activity Connection

L_x vs *vsin I*

Pallavicini et al. 1981, ApJ, 248, 279.

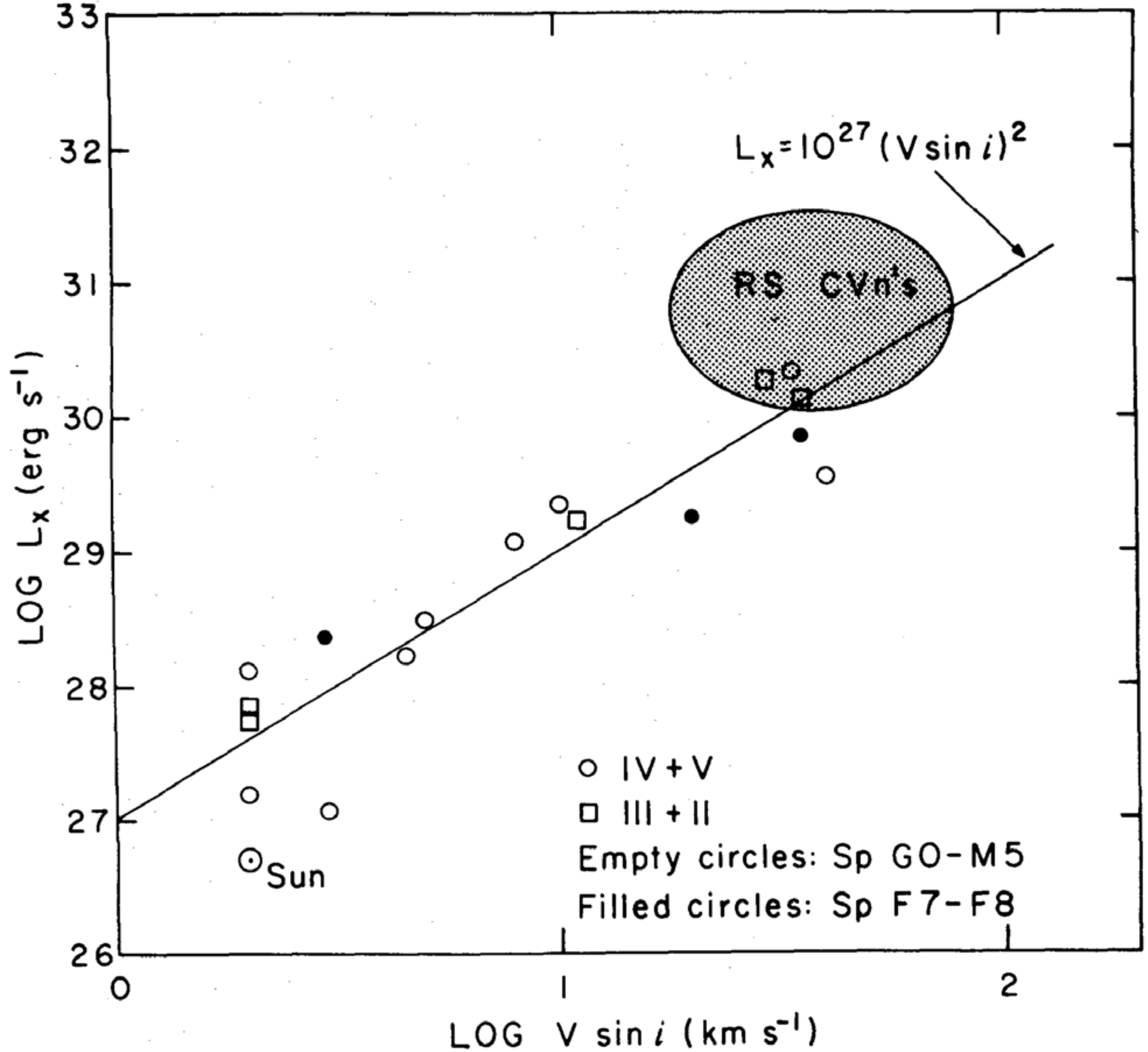

恒星と活動～彩層･コロナ～

R'_{HK} vs R_o

Noyes et al. 1984, ApJ, 279, 763.

$R_o \sim \Omega \tau_c$

R_o Rosby number

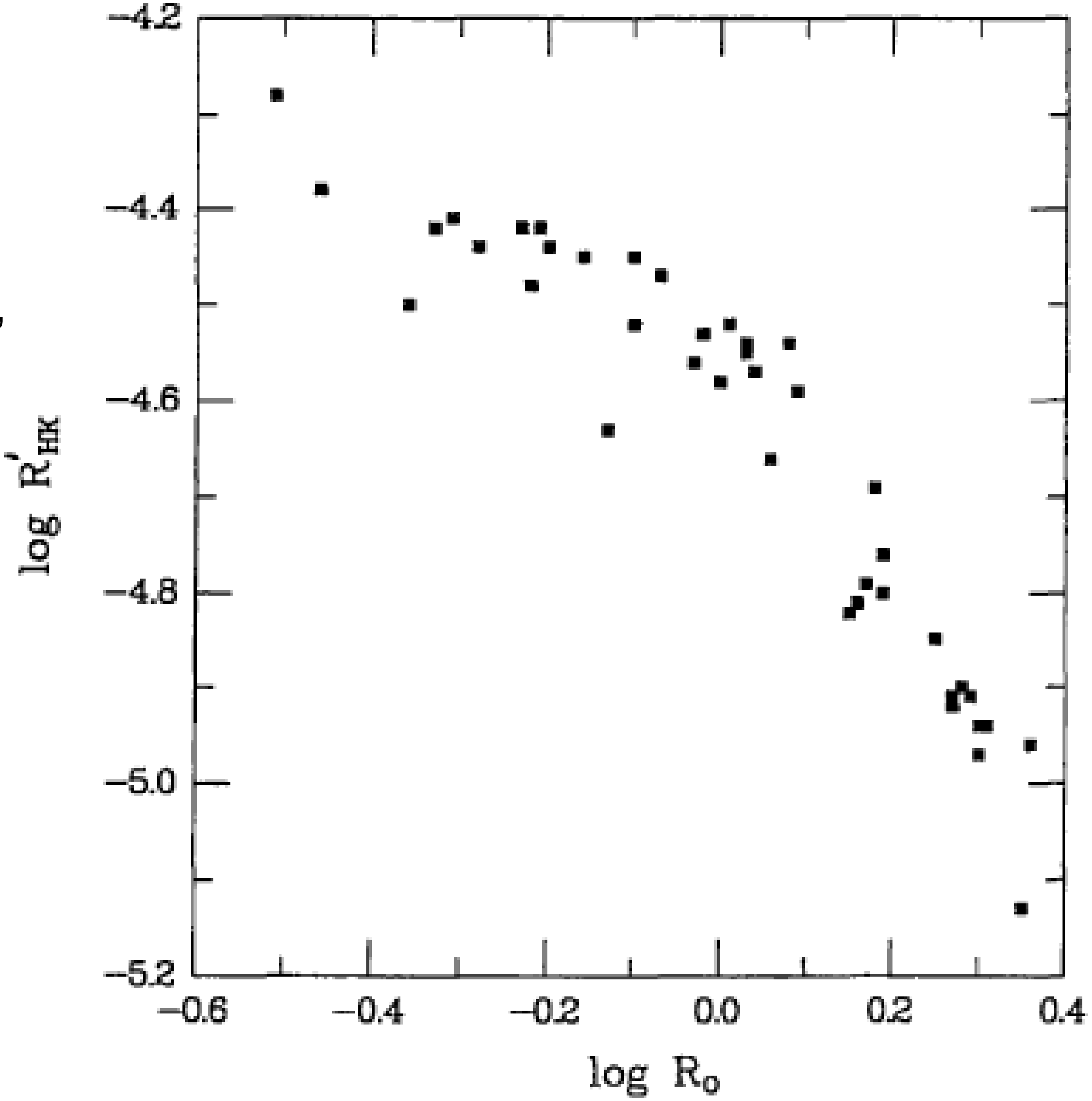

恒星と活動～彩層･コロナ～

S-index, R_{HK}, R'_{HK}

- Vaughan, Preston, Wilson (1978)
  - $S \sim H/(H_V+H_R) + K/(K_V+K_R)$
- Middelkoop (1982) : color correction
  - $R_{HK} \sim F_{HK}/(\sigma T^4_{eff})$
- Noyes et al. (1984): photospheric contr.
  - $R'_{HK} = R_{HK}-R_{photo}$

恒星と活動～彩層・コロナ～

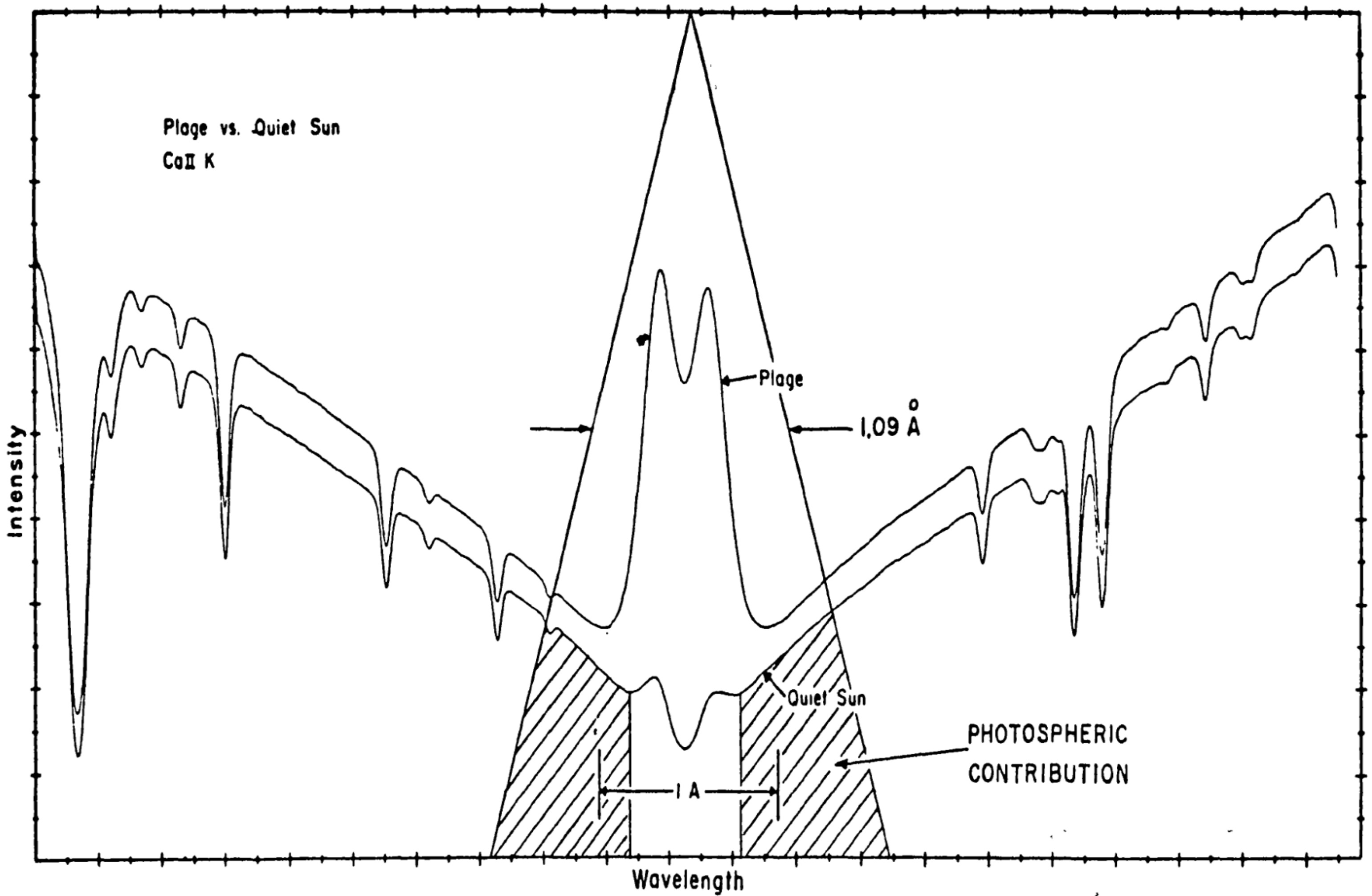

Figure 4 The K-line bandpass of the instrument used to produce the Vaughan-Preston (1980) survey and other Mount Wilson Ca II HK flux measurements, superimposed on both quiet Sun and plage spectra (Hartmann et al. 1984b).

恒星と活動～彩層･コロナ～

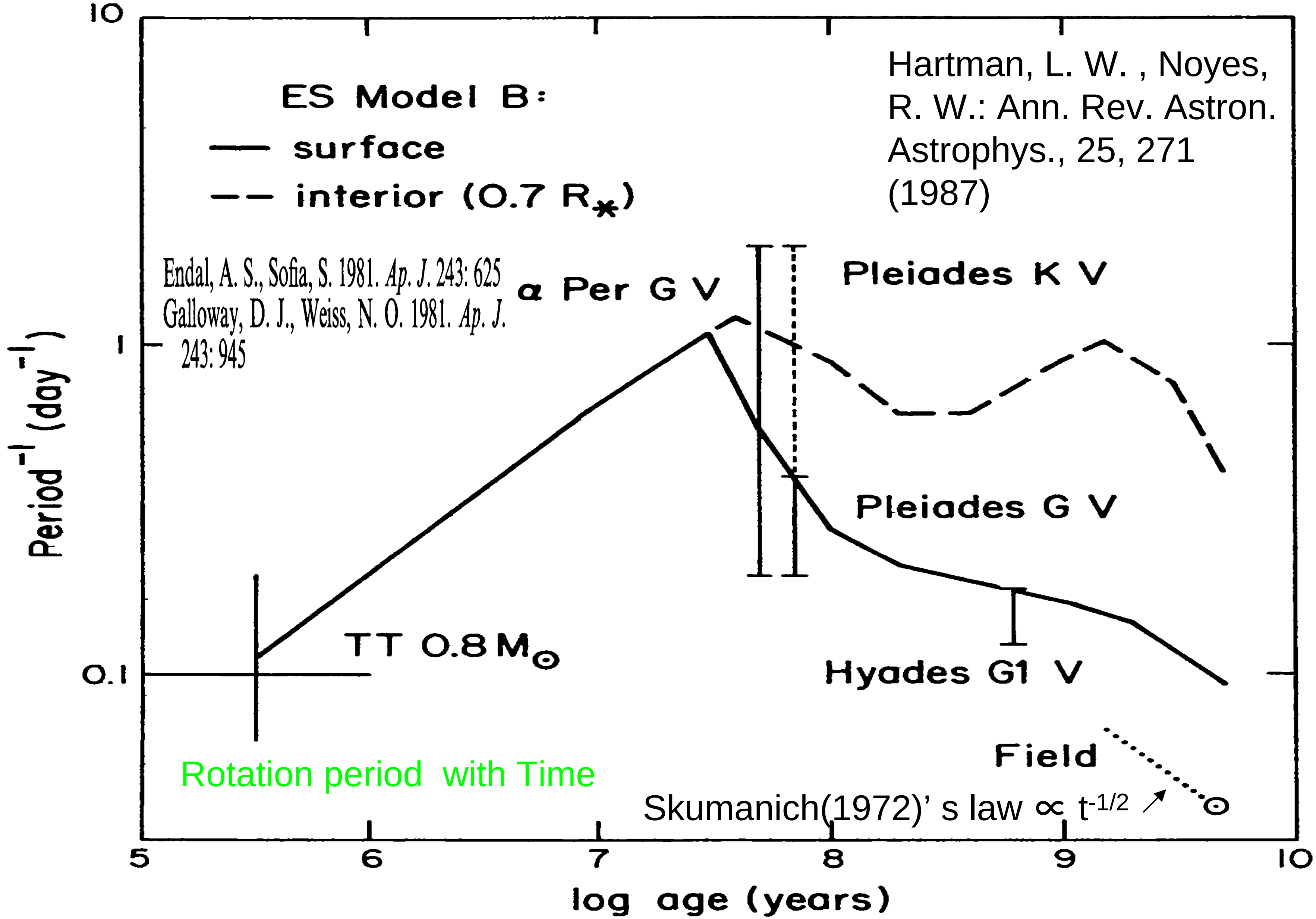

Hartman, L. W. , Noyes, R. W.: Ann. Rev. Astron. Astrophys., 25, 271 (1987)

恒星と活動～彩層・コロナ～

恒星活動

黒点・磁場

恒星と活動～彩層･コロナ～

Starspot –obs tech-

- Light-curve inversion
  - $I_i = f_i\ I_s + (1- f_i)I_p$ f_i: filling factor $0 \leqq f_i \leqq 1$
- Doppler imaging (Goncharskii et al. 77…)

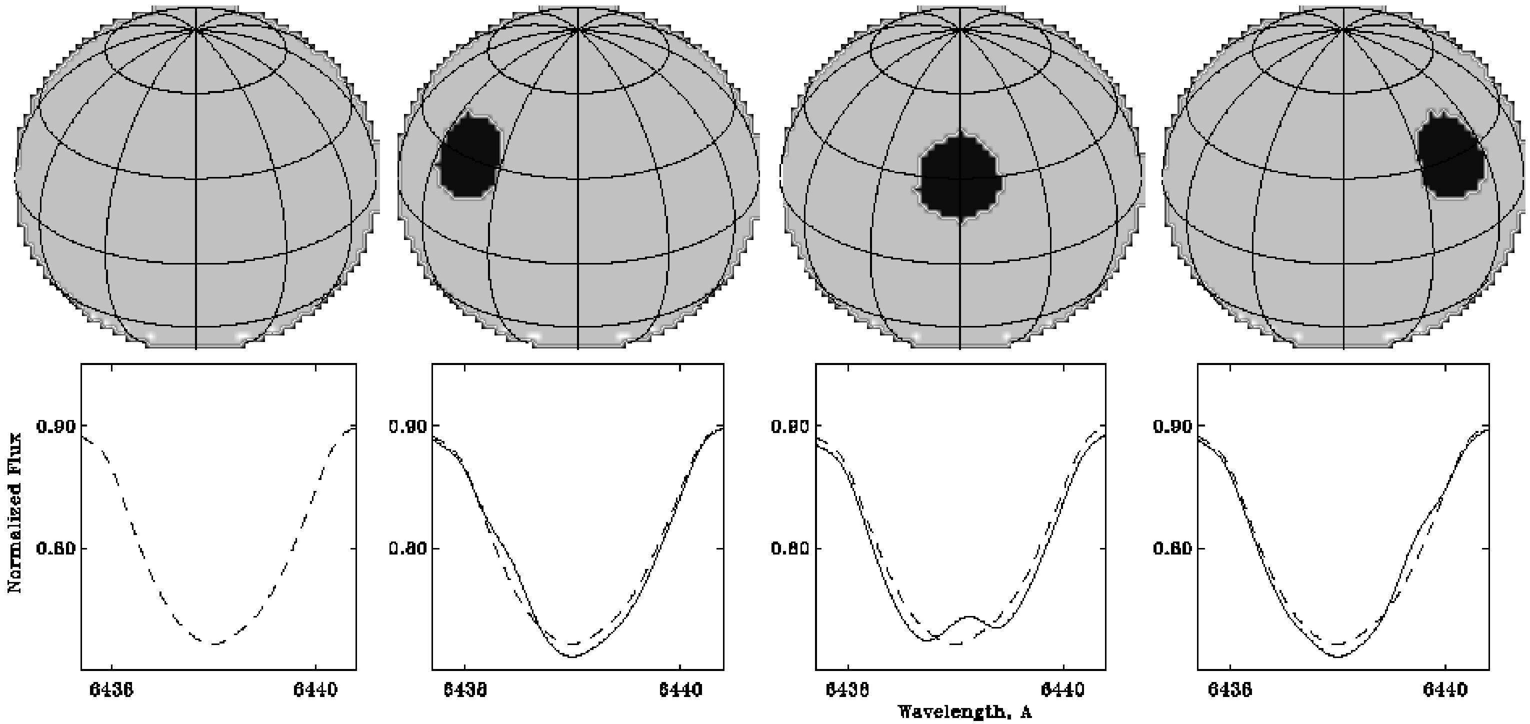

恒星と活動～彩層･コロナ～

Berdyugina, 2005, Living Rev. Solar Phys., 2, 8.

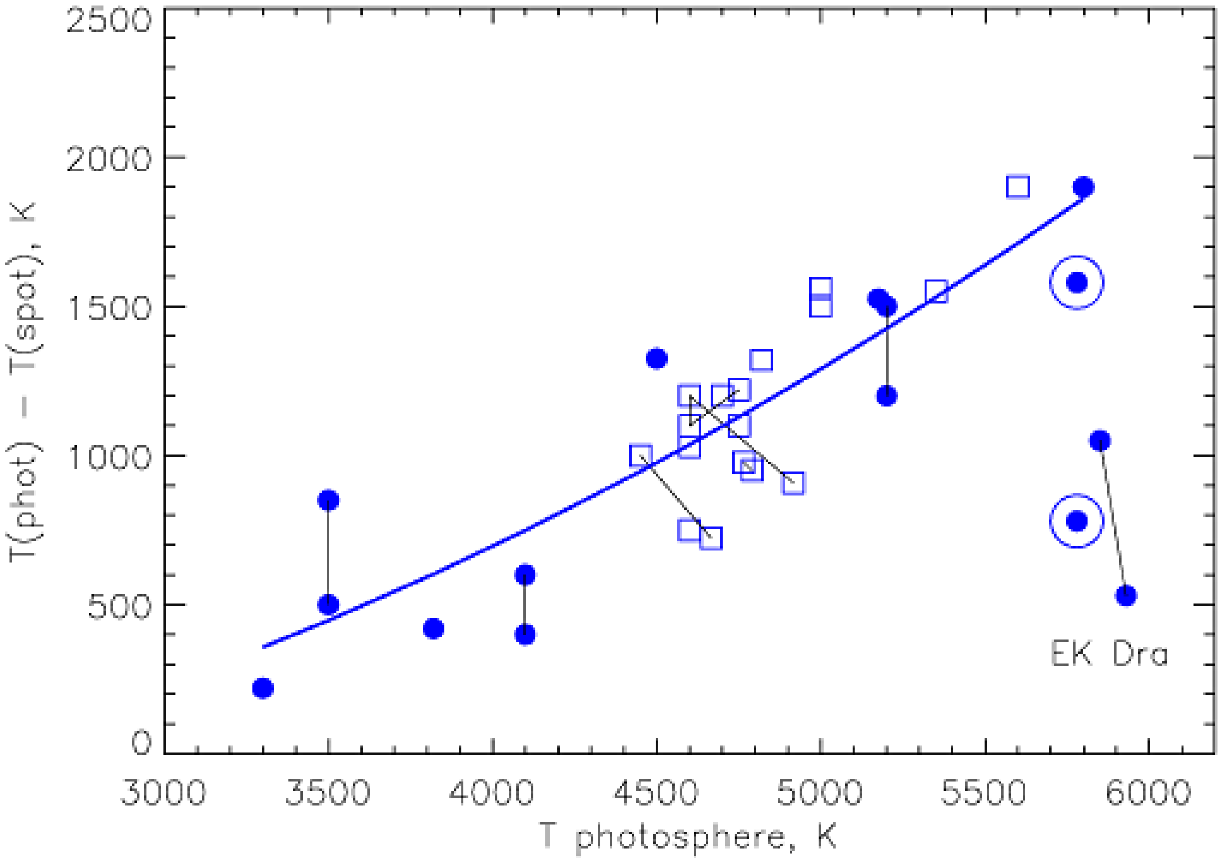

Spot temperature contrast with respect to the photospheric temperature in active giants (squares) and dwarfs (circles). Thin lines connect symbols referring to the same star. The thick solid line is a second order polynomial fit to the data excluding EK Dra. Dots in circles indicate solar umbra (T = 1700 K) and penumbra (T = 750 K) .

恒星と活動～彩層･コロナ～

Stellar Magnetic Fields –obs tech-

Robinson Jr., R. R. (1980)

Zeeman triplet:

$$\Delta\lambda(\text{Å}) \propto 4.7\times10^{-13} g \lambda^2 B\ (G)$$

（g：ランデのg因子）

$$F_\lambda = (1-f)\ F_\lambda\ (B=0) + f\ F_\lambda (B\neq0)$$

恒星と活動～彩層･コロナ～

Stellar Magnetic Field Measurements

(Berdyugina, 2005, Living Rev. Solar Phys., 2, 8.)

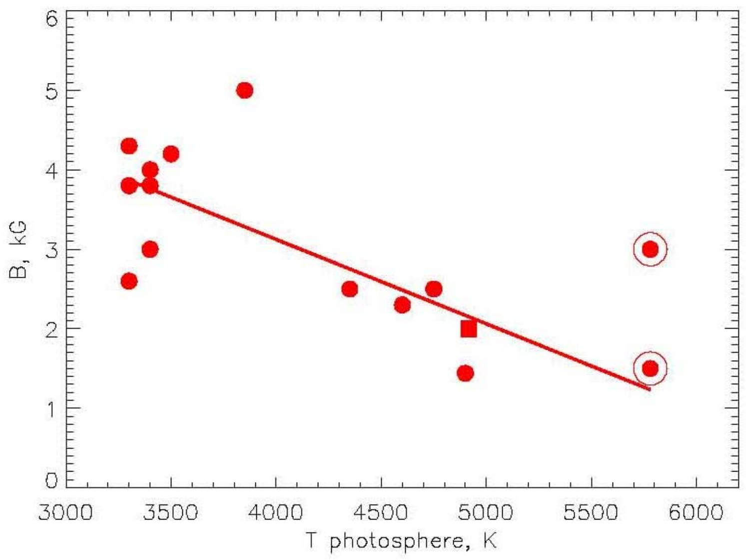

Magnetic field measurements for active dwarfs (circles) and giants (squares) versus the photosphere temperature. Big circles indicate the sunspot umbra (B = 3 kG) and penumbra (B = 1.5 kG). The thick solid line is a linear fit to the data, excluding the sunspot umbra.

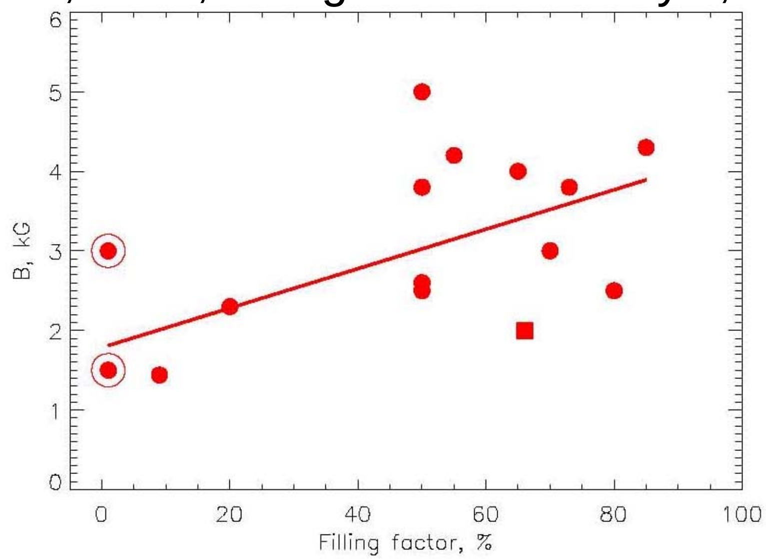

Magnetic field measurements for active dwarfs (circles) and giants (squares) versus the filling factor. Big circles indicate the sunspot umbra (B = 3 kG) and penumbra (B = 1.5 kG). The thick solid line is a linear fit to the data, excluding the sunspot umbra

恒星と活動～彩層･コロナ～

Filling Factors

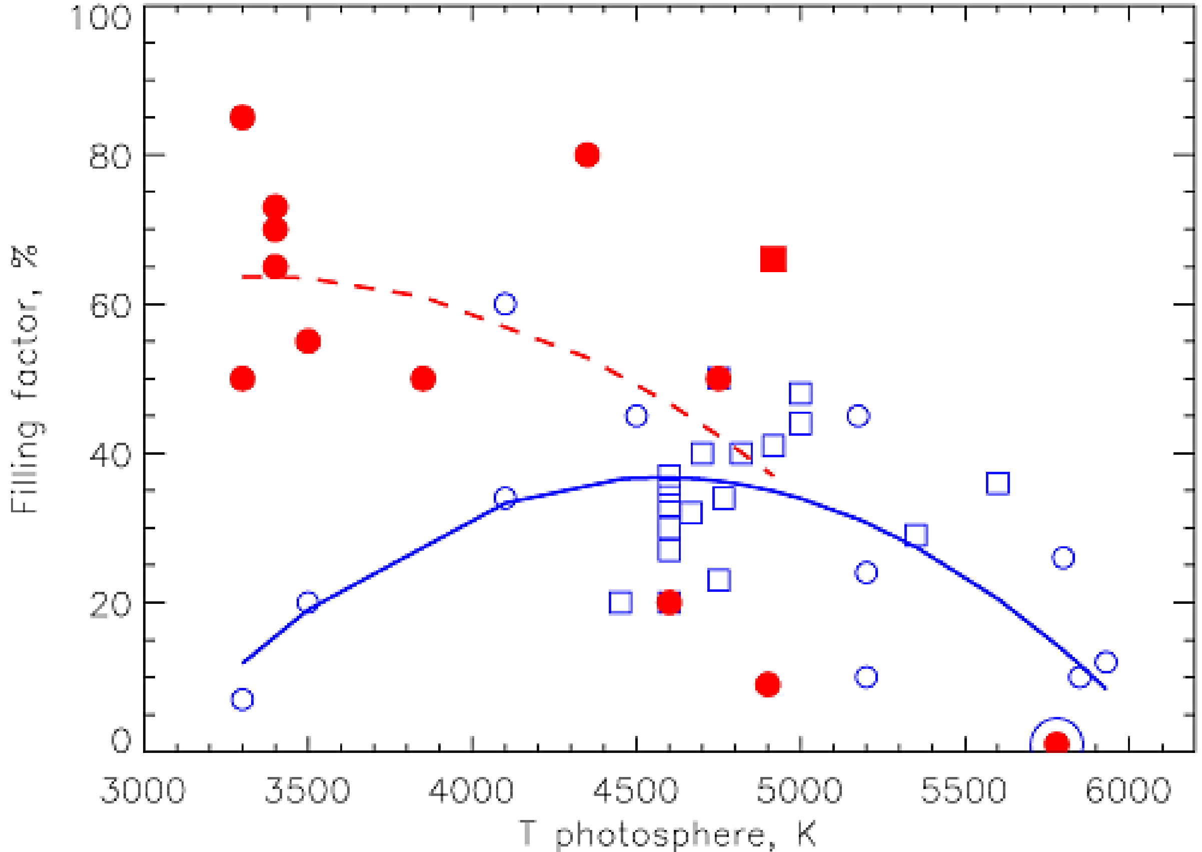

Filling factors of spots (open symbols) and magnetic fields (filled symbols) on the surfaces of active dwarfs (circles) and giants (squares) versus the photosphere temperature. The thick solid line is a polynomial fit to the spot filling factors. The dashed line is a fit to the magnetic field filling factor, excluding the Sun. A big circle emphasises the sunspot umbra (f ~1%).

(Berdyugina, 2005, Living Rev. Solar Phys., 2, 8.)

恒星と活動～彩層・コロナ～

恒星活動

周期活動

恒星と活動～彩層･コロナ～

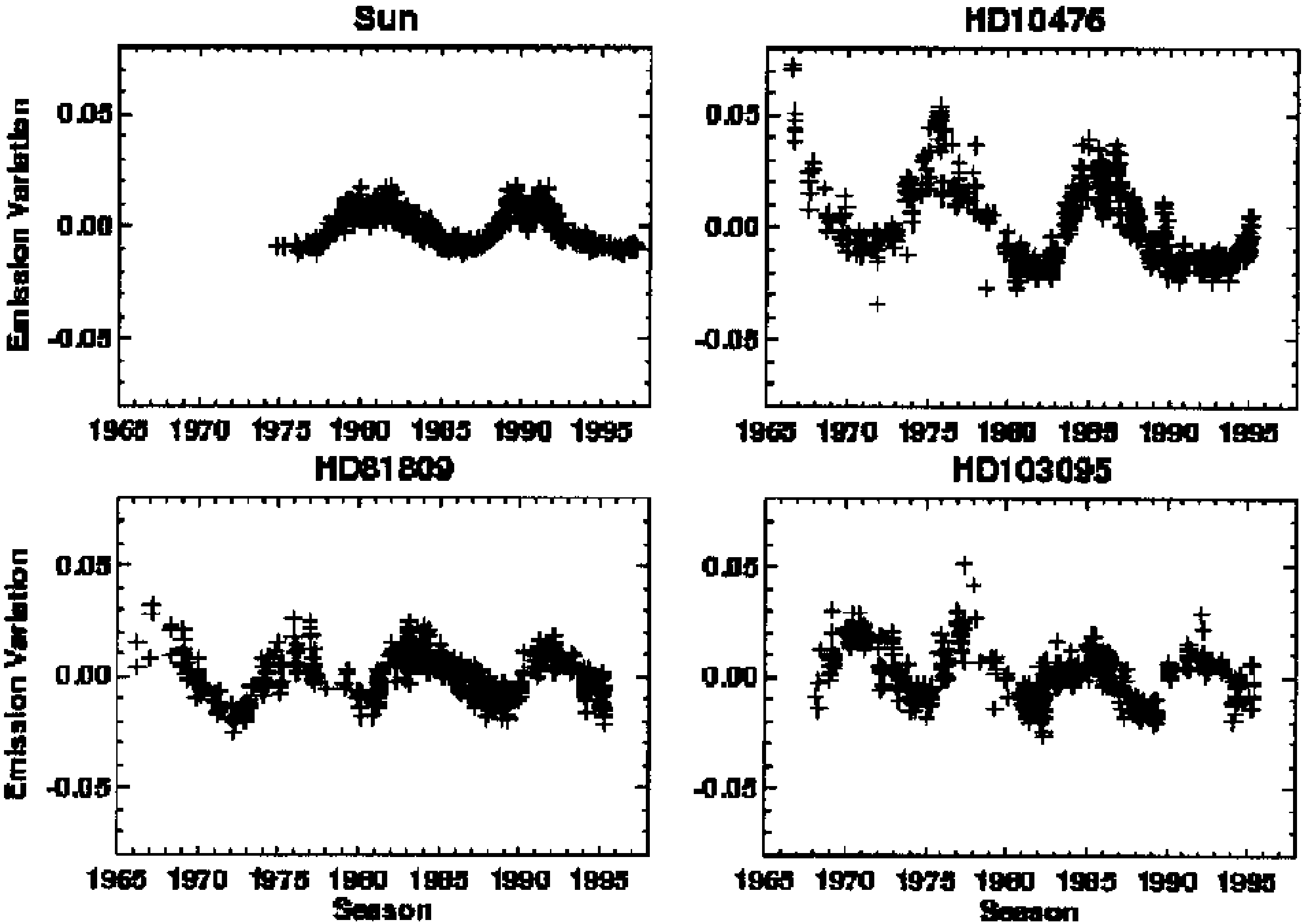

Chromospheric Ca II emission cycles for Sun-like stars, illustrating the regular cyclic variation that is common in such stars. The Ca II emission is plotted in Mount Wilson “S-Index” units. From Radick (2000).

恒星と活動～彩層･コロナ～

～100 Stars in spectral types of G0 - K5 V

- Young rapidly rotating stars
  - high average levels of activity
  - non-smooth cyclic variation.
- Stars of intermediate age (approximately 1 – 2 Gyr for 1M)
  - moderate levels of activity
  - occasional smooth cycles.
- Stars as old as the Sun and older
  - slower rotation rates
  - lower activity levels and smooth cycles.
- Stars of no variations
  - in the stage similar to the Maunder minimum
  - subgiants evolved off the main-sequence (Wright, 2004).
- vs. H/K chromospheric variation
  - young stars: anticorrelates with their variation in chromospheric emission → activity cycles on young stars should be more prominent in spot patterns rather than in chromospheric plages.

恒星と活動～彩層・コロナ～

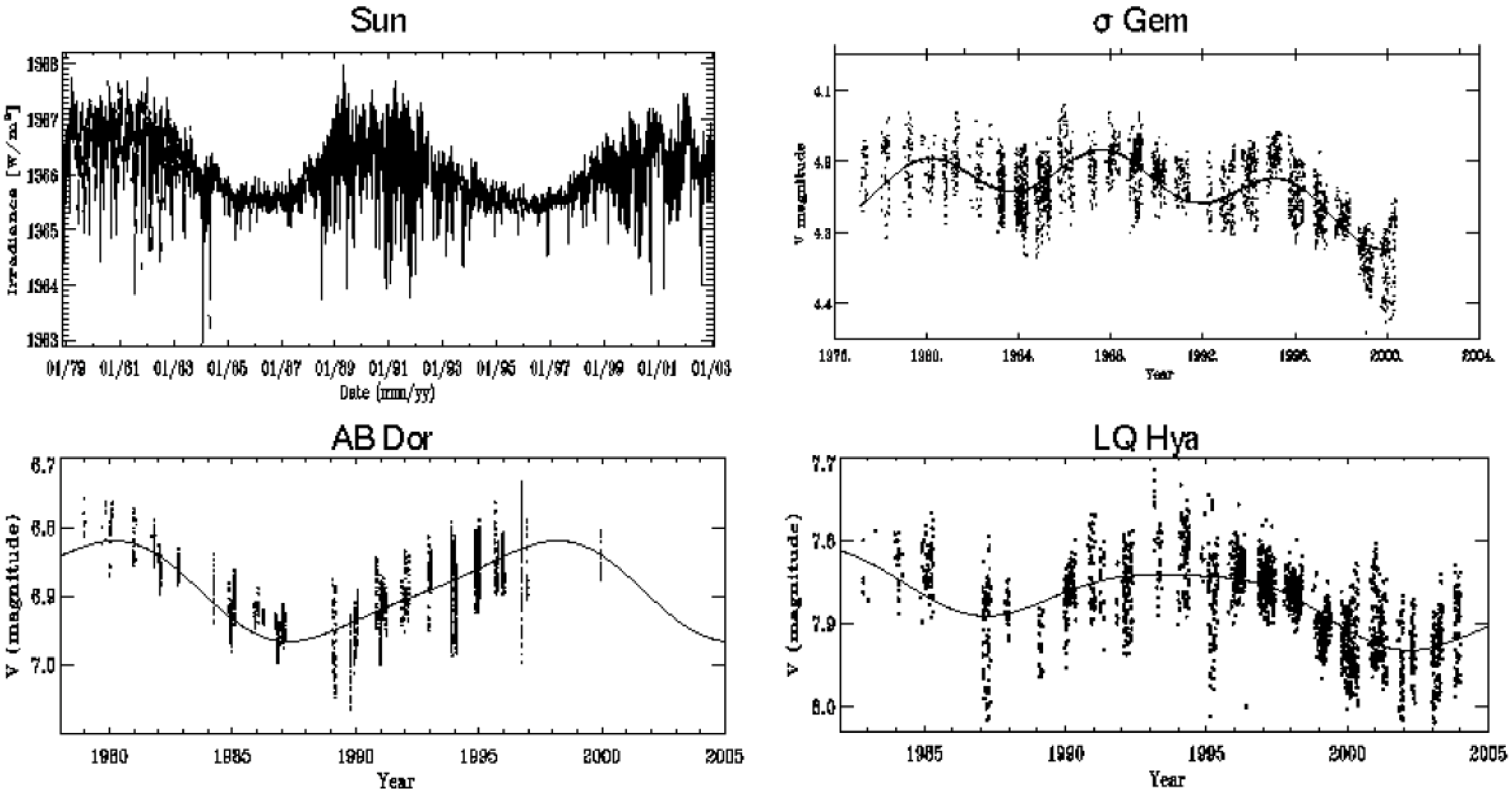

Spot cycles in the solar irradiance and V magnitudes of the RS CVn binary σ Gem and two young solar analogues AB Dor and LQ Hya. Note that the maximum of the spot area corresponds to the maximum irradiance on the Sun and minimum brightness on the stars.

恒星と活動～彩層･コロナ～

- Sun: maximum spot area at the maximum irradiance

- Active stars: maximum spot area at minimum brightness → periodic changes of spot rotation periods in phase with the spot cycle